PREPARATION AND EVALUATION OF CURCUMIN LOADED LYOPHILIZED WAFER FOR WOUND HEALING

THESIS SUBMITTED FOR THE DEGREE OF

MASTER OF PHARMACY

JADAVPUR UNIVERSITY

2024

By

SAMRAT CHOWDHURY

Roll No. – 002211402032

Examination Roll No. – M4PHL24006

Registration No. – 163674

DEPARTMENT OF PHARMACEUTICAL TECHNOLOGY

FACULTY OF ENGINNERING AND TECHNOLOGY

JADAVPUR UNIVERSITY

KOLKATA – 700032

INDIA

JADAVPUR UNIVERSITY

KOLKATA – 700032

Title of the thesis

PREPARATION AND EVALUATION OF CURCUMIN LOADED LYOPHILIZED WAFER FOR WOUND HEALING

Name, Designation and Institution of the supervisor:

Dr. Kajal Ghosal, Assistant Professor

Department of Pharmaceutical Technology

Jadavpur University

Kolkata – 700032, India.

DEPARTMENT OF PHARMACEUTICAL TECHNOLOGY

FACULTY OF ENGINEERING AND TECHNOLOGY

JADAVPUR UNIVERSITY

CERTIFICATE OF APPROVAL

This is to certify that the thesis entitled "**PREPARATION AND EVALUATION OF CURCUMIN LOADED LYOPHILIZED WAFER FOR WOUND HEALING**" submitted by **Samrat Chowdhury**, of Jadavpur University, for the course of **Master of Pharmacy** is absolutely based upon his work under the supervision of **Dr. Kajal Ghosal**, Assistant Professor, Department of Pharmaceutical Technology, Jadavpur University, Kolkata and that neither his thesis nor any part of the thesis has been submitted for any degree/diploma or any other academic award anywhere before.

Kajal Ghosal 29/8/2024

Dr. Kajal Ghosal
Assistant Professor
Department of Pharm. Tech
Jadavpur University
Kolkata - 700032

(Signature of M.Pharm thesis Guide)

Asst. Prof. Kajal Ghosal

Department of Pharmaceutical Technology

Jadavpur University, Kolkata – 700032.

29.8.24.

Head
Department of Pharmaceutical Technology
Jadavpur University
Kolkata - 700 032, W.B. India

(Signature of Head of the Department)

Prof. (Dr.) Amalesh Samanta

Department of Pharmaceutical Technology

Jadavpur University, Kolkata – 700032.

Dipak Laha 29.8.24

(Signature of Dean)

Faculty of Engineering and Technology

Jadavpur University, Kolkata – 700032.

DEAN
Faculty of Engineering & Technology
JADAVPUR UNIVERSITY
Kolkata 700 032

DECLARATION BY THE CANDIDATE

I do hereby declare that the work incorporated in the thesis entitled **"PREPARATION AND EVALUATION OF CURCUMIN LOADED LYOPHILIZED WAFER FOR WOUND HEALING"** has been carried out by me in the Department of Pharmaceutical Technology, Jadavpur University under the supervision of Dr. Kajal Ghosal, Assistant Professor, Department of Pharmaceutical Technology, Jadavpur University, Kolkata – 700032. Neither the thesis nor any part therefore has been submitted for any other degree.

Samrat Chowdhury

Date: 29.08.24

Signature of the candidate

Place: Kolkata, India

(SAMRAT CHOWDHURY)

.

Dedicated to my Guide and My Family

ACKNOWLEDGEMENT

I would like to extend my heartfelt gratitude to several individuals who have played pivotal roles in the successful completion of my thesis. First and foremost, I extend my heartfelt thanks to my guide, Dr. Kajal Ghosal for her unwavering guidance, invaluable insights, and continuous support throughout my research journey. Her mentorship has been instrumental in shaping my work.

I am also immensely grateful to Dr. Jasmina Khanna for generously sharing her wealth of knowledge for my project work. Her generosity has significantly enriched my research experience.

I am also grateful to Prof. Amalesh Samanta , Head of the Department of Pharmaceutical Technology at Jadavpur University, and all the esteemed faculty members of the department for their individual guidance, valuable suggestions, and kind cooperation.

I offer special gratitude and unfeigned thanks to my lab partner, Mr. Souvik Singha for his unwavering assistance, which has been a constant source of support throughout my research. I wish to express my deepest appreciation to my senior, Mrs. Shreya Chatterjee, and my juniors, Mr. Somnath Singha and Mr. Puspendu Singha, for creating a congenial and collaborative environment, providing kind support, actively participating in project-related discussions, and offering encouragement throughout my research journey. I am indebted to all my friends at Jadavpur University who have directly or indirectly contributed to the progress of my research work.

My heartfelt gratitude extends to all the non-teaching staff of the Department of Pharmaceutical Technology for their invaluable support. To all those mentioned and many more who have supported, guided, and encouraged me during this journey, I extend my deepest gratitude. Your contributions have been indispensable in the realization of this work.

Last but not least, I gratefully acknowledge my parents, my beloved sisters, and my relatives for their unwavering encouragement, moral support, limitless blessings, and their constant presence in my life, which have enabled me to reach this significant milestone.

Date: SAMRAT CHOWDHURY

PREFACE

The thesis presented here, titled "**PREPARATION AND EVALUATION OF CURCUMIN LOADED LYOPHILIZED WAFER FOR WOUND HEALING**" delves into the intricate realm of synthesizing magnetite using the co-precipitation method. Additionally, this research endeavors to create magnetic beads loaded, with the primary objective of facilitating targeted drug delivery while mitigating the potential side effects associated with drug administration.

- Chapter 1 introduces the fundamental concepts topical drug delivery system and how skin metabolism of drug takes place. Advantages and disadvantages of TDDS were further included in the discussion. Different forms of topical drug delivery system with special emphasis Lyophilized wafer was briefed. Various stages of wounds, process of wound healing along with different phyto-constituents used for wound healing were discussed.
- Chapter 2 presents a comprehensive literature survey on the relevant subject matter.
- In Chapter 3, the aims and objectives are outlined.
- Chapter 4 catalogs the materials utilized in the project.
- Chapter 5 encompasses the procedures for Lyophilized wafer preparation, the pre-formulation studies of the drug along with a description of the characterization techniques employed.
- Chapter 6 delves into the presentation and discussion of the results.
- Chapter 7 offers a summary and conclusion of the present work.
- And finally, Chapter 8 provides the reference of the work done.

CONTENTS

LIST OF FIGURES:

LIST OF TABLES:

	formulation.
7	shows folding endurance of Blank, F1,F2 and F3 formulation
8	Shows the percentage yield (%) of Blank, F1, F2 and F3 formulation.
9	CDR% Calculation for F1 formulation.
10	CDR% Calculation for F2 formulation.
11	CDR% Calculation for F3 formulation.
12	Shows summary of R^2 value of different release kinetics model.
13	Calculation of zero order kinetics.
14	Calculation of first order kinetics.
15	Shows calculation of HIGUCHI model release kinetics
16	Shows calculation of HIXSON-CROWELL model release kinetics
17	Shows calculation of KORSMEYER-PEPPAS model release kinetics

CHAPTER 1:

INTRODUCTION

1. INDRODUCTION

1.1. INTRODUCTION TO TOPICAL DRUG DELIVERY SYSTEM

Skin disorders are a major contributor to the global illness burden, impacting millions of individuals globally. A wide range of skin illnesses, with over 3000 entities recognized in the literature, can arise from a combination of environmental, genetic, traumatic, and aging causes. Skin illnesses can have acute or persistent symptoms, which vary in intensity. Individuals undergoing immunosuppressive medication and those with illnesses like diabetes are particularly vulnerable to opportunistic skin infections. Numerous skin conditions might result from systemic disease's surface symptoms. Skin problems can range in severity from trivial to potentially fatal. Acne, eczema, seborrhea dermatitis, psoriasis, urticaria, skin cancer, and fungal, bacterial, viral, and parasite skin infections are common skin illnesses.

The topical administration of medications is used to treat a variety of skin conditions. In most circumstances, oral administration is advised in addition to topical treatment since topically applied medications do not penetrate the skin well enough to produce concentrations high enough to demonstrate pharmacological effects. Orally administered medications, however, have a wide range of adverse effects because of their nonspecific dispersion throughout the body. For this reason, topical drug application is preferred over oral drug administration because there is a lower risk of systemic adverse effects and consequences from restricted systemic exposure. [1] Thus the skin is treated with topical preparation for systemic, local, or surface effects. Sometimes, the base might be utilized exclusively for its medicinal properties, like a soothing, emollient, or protecting effect. However, a lot of topical medicines include components that are dissolved or disseminated in the base and have therapeutic effects.

The combination of the active components and base allows for a variety of topical formulations that can be used for different kinds of medication administration. Topical sprays and foams, topical peels, occlusion (via dressings and patches), bio-polymers (e.g., sodium hyaluronate), liposomes, particulate carriers (microspheres and lipid nanoparticles), temperature (heat), iontophoresis, and ultrasound are some of the current and emerging methods for optimizing the topical delivery of dermatological agents (small and large molecules). These delivery methods are a significant advancement over traditional systems (creams, lotions, ointments, and pastes) when used alone or in combination. They may also

improve patient compliance (including the quality of dermatological life), increase efficacy and tolerability, and meet other unmet needs in the topical dermatology market.

Several of the novel biologics-based medications and vaccines could be administered topically via dermal and transdermal delivery systems, which having important advantages, can replace the use of needles. [2]

1.1.1. ANATOMY OF SKIN

The largest organ, the skin is complex and multipurpose, with several specialized cells that are tailored to various tasks. The epidermis, the outermost layer of skin, is tightly adhered to the dermis, the innermost layer, by means of the basement membrane. The dermis is composed of fat and loose connective tissue.

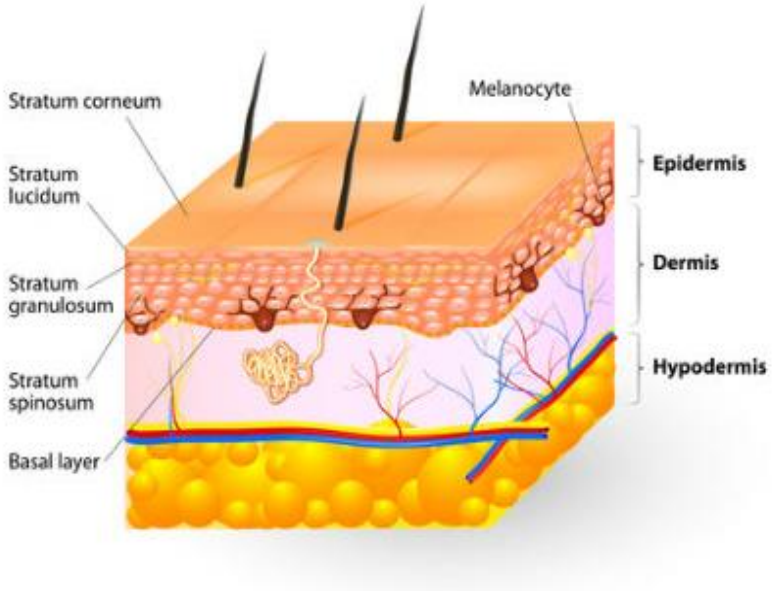

Figure 1: Anatomy of skin: Epidermis, Dermis and Hypodermis [3]

- **Epidermis**: The "basal" cell layer, which is a single sheet of columnar cells at the lowest level of the epidermis, divides to generate layers of densely packed cells that make up the stratified squamous epithelium that makes up the epidermis. Thirty percent of these columnar cells are always preparing to divide. One cell stays in place after division, carrying out the functions of adhesion to the basement membrane, replication, and repair. The other cell goes suprabasally, differentiating into a keratinocyte while being unable to divide. It is forced upward through the granular

and spinous layers as additional cells are produced from the basal layer, eventually arriving at the horny layer, where it is shed. In normal skin, the time interval between cell division and shedding is 28 days. Skin thickness varies depending on function; for example, it is 0.1 mm thick over eyes and 2 mm thick over foot soles.

- **Dermis**: Beneath the epidermis, the dermis provides structural and nutritional support for it. Fibroblasts and the collagen they generate make up the majority of it. The triple helix that makes up collagen is made up of three polypeptide chains. Bundles of fibers have a tremendous tensile strength. Stretching elastin fibers are also seen in the dermis.

  A matrix of amorphous mucopolysaccharide ground material surrounds the fibers. This functions as a lubricant to permit skin movement, binds water to assist the transport of nutrients and other substances, and adds weight to help absorb shock.[4]

- **Subcutaneous fat**: Beneath the reticular layer of the dermis, subcutaneous tissue is composed of looser connective tissue. It then turns into subcutaneous adipose tissue. The location, sex, and nutritional status of the adipose cells determine the thickness of the layer they create. Adipose tissue serves as a shock absorber and aids in energy storage and thermal insulation. It permits the skin to glide over the underlying deep fascia, the aponeurosis or the periosteum, and loosely connects them. The subcutaneous area of the penis, clitoris, and eyelids is devoid of adipose tissue. The hypodermis contains a sizable capillary network that is part of the vascular system. It enables the quick absorption of medications administered subcutaneously, particularly insulin. [5]

1.1.2. METABOLISM OF DRUG THROUGH SKIN

The key enzymes that catalyze various metabolic events and are present in the liver and other tissues are all present in the skin. The chemical compounds applied topically undergo metabolic changes that alter their pharmacological and toxicological effects. But it has been shown that the skin's enzyme activity is lower than the liver's. Therefore, the skin may serve as a portal for the body's absorption of medication compounds. Many chemical groups, including alcohols, acids, primary amines, esters, and others, are especially vulnerable to skin metabolism. Several drug-metabolizing enzymes, such as epoxide hydrolase, CYPs,

transferases (N-acetyl transferases), glucuronyl transferases, and sulfatases, are present in the viable dermis.

In vitro permeation studies utilizing living skin can be used to assess the skin metabolism, or metabolites can be detected in skin homogenate or receptor fluid.

The absorption phase has been the subject of most dermatopharmacokinetic investigations. The fate of the molecule following absorption, although equally crucial in determining the topical formulations' bioavailability, has not been well explored. It is probable that the drugs with unique characteristics will reach the dermis, whereupon they will go to the systemic circulation through lymphatic or blood vessels of the dermis.

Topical medications and other chemicals' pharmacological effects are directly influenced by microvascular factors like blood flow rate. The skin's microenvironment is a dynamic component of the body that is always changing. The rich vascular network system in the skin controls and deals with a variety of skin functions.

The two horizontal plexuses that make up the cutaneous microvasculature are enclosed by the papillary dermis, which is located 1-2 mm below the epidermal surface. The lower plexus is situated around the dermal-hypodermal junction, which gives rise to arterioles and venules. The separation between the reticular and papillary dermis is represented by the second plexus, which is situated 1-2 mm below the skin's surface. [6]

1.1.3. DIFFERENT FORMS OF TOPICAL DRUG DELIVERY SYSTEM

Topical formulations include gels, ointments, creams, pastes, powders, shake lotions, ointments, and wet preparations. The kind chosen is determined by a number of variables, including the qualities of the skin condition, the patient's overall skin type, the effects of prior medications, and drug allergies. [7]

- **Creams**:

The use of cream formulations as effective means of delivering medications and cosmetic ingredients to the skin is becoming more and more popular. These are referred to as biphasic systems because they are made up of two immiscible liquids, one of which is uniformly distributed throughout the other to create emulsions that are either water-in-oil (w/o) or oil-

in-water (o/w). These are intriguing formulations that can be used to deliver medications that are both lipophilic and hydrophilic. [8]

- **Ointment**:

Ointments are made of a hydrophilic greasy basis, typically white soft paraffin, that creates an occlusive layer on the skin to stop heat and moisture loss. By raising the skin's warmth and moisture content, they effectively improve the topical corticosteroid's absorption via the skin. Ointments have the lowest spreadability of the three, when compared to creams, lotions, and solutions. Because ointments' oily texture can often make patients less compliant, especially on skin that bears hair, their galenic qualities are not necessarily cosmetically pleasing. [9]

- **Gel**:

Gels are transparent lattices of organic macromolecules thickened with cellulose derivatives. They are prepared as a colloidal dispersion of water, acetone, alcohol, or propylene glycol. Their usefulness as an occlusive emolliating medium is limited because they are transparent semisolid emulsions that liquefy when in contact with warm skin and dry as a greaseless nonocclusive film. They are therefore especially well-suited for the treatment of diseases of the scalp like psoriasis. The fact that perspiration eliminates the gel from gel vehicles is one of their major limitations. [9]

- **Liniment:**

It is used topically to ease aches and pains in the muscles.
Certain ingredients in it create minor irritation when rubbed to the targeted skin area, and frequently increase blood flow to the sore area. The majority of liniments include wintergreen, turpentine, or camphor oils. In wintergreen, methyl salicylate is the primary ingredient. It is used medicinally to lessen fever, headaches, and menstruation pain. It is also used in liniments to relieve aches in the muscles. [10]

- **Paste:**

Pastes are composed of a blend of several powders and ointments.
To prevent dust inhalation during application, powdered pharmaceuticals or ointments can be made into pastes. This makes them more difficult to remove from the skin.
One excellent example of a paste that is challenging to just wipe away is zinc oxide, which is used in diaper rash creams. Oral wounds can also be treated with pasted topicals since they

adhere to the mucous membranes and provide a barrier that is difficult for saliva to remove; which is ideal for the treatment of canker sores. [11]

- **Transdermal film:**

A transdermal film, adhesive patch, or skin patch is used to gradually provide a controlled dosage of medication through the skin. The pace at which the liquid medication in the reservoir of a skin patch can permeate the skin and enter the bloodstream is regulated by a unique membrane. For certain pharmaceuticals to be utilized in a skin patch, they need to be mixed with materials like alcohol that make them more soluble in the skin. [12]

- **Lyophilized wafer:**

Lyophilized wafers are among the most sophisticated dressing for administering drugs to wounds. Wafers' exceptional porosity allows them to retain moisture and absorb enormous volumes of heavy exudate without harming the newly created tissue that speeds up wound healing. Because of the wafers' porosity, gaseous (water vapour) exchange is also made possible, allowing wound exudates to evaporate into the surrounding air through the polymeric matrix and prevent fluid build-up under the dressing. This lowers the risk of skin maceration and also controls infections. [13]

Lyophilized wafers are formulations that are made by freeze-drying gels and polymeric solutions to create solid structures that are porous in nature and are easily applied to wounded exudating surfaces.

Chronic wounds that produce a lot of exudate, including diabetic foot and venous ulcers, restrict the use of transdermal film dressings. Due to their inability to absorb large amounts of exudate, film dressings force the fluid to accumulate beneath them, which leads to maceration at the wound site and necessitates frequent dressing changes that have a negative impact on patient compliance.[14]

Owing to their incapacity to absorb large volumes of exudates, current dressings for chronic Diabetic Foot Ulcers treatment, such as hydrogels, hydrocolloids, and films, are typically incapable of treating Diabetic Foot Ulcers effectively in all circumstances. Conversely, upon removal, foam, gauze, bandages and sponges can contribute to discomfort and anguish for the patient. Because of their adhesion to the wound, which causes debridement and slows down the healing process, these dressings can also result in dermatitis.

Exudate from chronic ulcers, like Diabetic Foot Ulcers, typically produces large volumes of exudate, and this collection of exudate under a dressing can macerate the surrounding healthy skin and create an environment that is favourable for infection. Because of the lyophilized wafers' porosity, gaseous (water vapour) exchange is also made possible, allowing wound exudates to evaporate through the polymeric matrix and into the surrounding air. This process lowers the risk of skin maceration and infection control by preventing fluid build-up under the dressing. [15]

1.1.4. ADVANTAGES AND DISADVANTAGES:

Advantages of topical drug delivery system:

The pharmaceutical industry is always changing, and one of the most notable developments in recent times has been the introduction of topical drug delivery methods. Numerous advantages provided by these technologies have changed the way that medical treatments are provided.

- **Targeted Treatment:** The capacity of topical drug delivery to offer tailored treatment is arguably its greatest benefit. Topicals are administered directly to the site of action, as opposed to oral drugs, which travel throughout the body. By minimizing the amount of the medicine that is exposed to healthy tissues, this accuracy lowers the possibility of side effects and improves the therapeutic result.

- **Localized Impact**: Localized effects are best provided by topical medication administration. For example, skin problems can be treated directly without interfering with other body systems. This is especially helpful when a drug's systemic absorption could have unintended side effects.

- **Diminished Systemic Adverse Effects:** Topical medications greatly reduce the risk of systemic adverse effects by avoiding the gastrointestinal tract and utilizing the liver for first-pass metabolism. For individuals who may be more vulnerable to the side effects of systemic drugs, this is especially beneficial.

- **Patient compliance:** When compared to oral prescriptions, topical therapies are typically easier for patients to apply and require less frequent administration, making

them more convenient overall. Better patient adherence to recommended regimens may result from this.

- **Non-Invasive Route:** Because topical medication distribution is non-invasive, it is particularly advantageous for people who may have trouble swallowing pills or who are uncomfortable with injections. Patient compliance and comfort are improved by this feature.

- **Potential Controlled Release route:** Some topical formulations—such as patches—allow for the gradual, controlled delivery of medication over a predetermined time frame. As a result, there is less need for frequent dosage and the medication concentration in the body is more constant, ensuring a continuous therapeutic impact.0

- **Appropriate for critical Skin Conditions:** Dermatological diseases are especially well-suited for topical administration. Acne, psoriasis, and eczema are examples of skin conditions that frequently need for the affected regions to be directly medicated. A straightforward and efficient method for treating these problems is through topical therapies.

- **Suitable for Particular Populations:** Topical delivery is adaptable and appropriate for a range of patient types, including elderly and pediatric patients. This is useful when giving medicine to people who might have trouble taking conventional oral drugs.

Topical Drug delivery techniques provide significant and evident benefits. Patient care has been completely transformed by this creative technique to drug administration, which offers tailored treatment, fewer systemic adverse effects, ease, and compatibility for different patient groups.[16]

Disadvantages of topical drug delivery system:

- Potential for localized skin irritation when the product is applied.

- It is possible to have drug-induced contact dermatitis.

- Certain medications possess limited permeability, making it challenging for them to permeate the skin.

- Drugs with bigger particles are harder to get through.
- The potential for an immunological response. [17]

1.2. TOPICAL DRUG DELIVERY SYSTEM AND WOUND HEALING PROCESS

1.2.1. TYPES OF WOUND HEALING

- **Primary wound healing**: When a wound is closed within 12 to 24 hours after its development (e.g., clean surgical incision, clean laceration), primary healing (healing by first intention) takes place. Through the use of tapes, sutures, tissue glue, or a mechanical device, the wound borders are immediately approached.

The incision only results in a small amount of epithelium and underlying connective tissue cell death and isolated disruption of the epithelial basement membrane's integrity. Consequently, epithelial regeneration outweighs fibrosis. Additionally, wounds heal efficiently and move quickly toward total closure because all stages of the healing process—including cellular proliferation, collagen metabolism, matrix metalloproteinase activity, and extracellular matrix degradation—are well balanced.

- **Delayed primary healing**: Infected or poorly defined wounds (such as bites and abdominal wounds following peritoneal soiling) that are closed after a few days in order to prevent infection are examples of wounds with delayed primary healing. After the host's defenses have assisted in debriding the wound, closure is carried out without causing anatomical trauma to the skin or subcutaneous tissues (sutures may be placed, but not fastened).

  After three to four days, the inflammatory cells eradicate the contaminating bacteria when phagocytic cells are locally recruited into the wound. Even after a few days have passed, the wound edges can still be roughly estimated. The collagen metabolism is mostly intact, and the wound keeps its tensile strength as if it had closed right away.

- **Secondary wound healing:** Secondary healing, also known as healing by second intention, happens when there has been a significant loss of soft tissue in the wound. This can happen after certain surgical procedures, such as a laparostomy, or major trauma.

  Since the original architecture cannot be restored only by epithelial cell regeneration, granulation tissue grows inward from the wound margin and accumulates extracellular matrix as collagen is laid down. Accordingly, these open, full-thickness wounds close as a result of subsequent epithelialization and wound contraction. For instance, major skin abnormalities can, mostly by contraction, shrink to 5–10% of their initial size in just six weeks.

Myofibroblasts are believed to be essential to this kind of repair because of their structural similarities to smooth muscle cells and fibroblasts. They first show up in the wound three days after it is inflicted, and between the tenth and twenty-first days, their number reaches its peak. Secondary intention healing is slower, more likely to result in functional restriction, and contractures, especially over joints. [18]

1.2.2. PROCESS OF WOUND HEALING

The phases of hemostasis, inflammation, and proliferation are all involved in the systemic process of wound healing. Fibrin production during hemostasis produces a shielding wound scab. The scab offers a surface on which the edges of the wound can shift and cells can migrate.

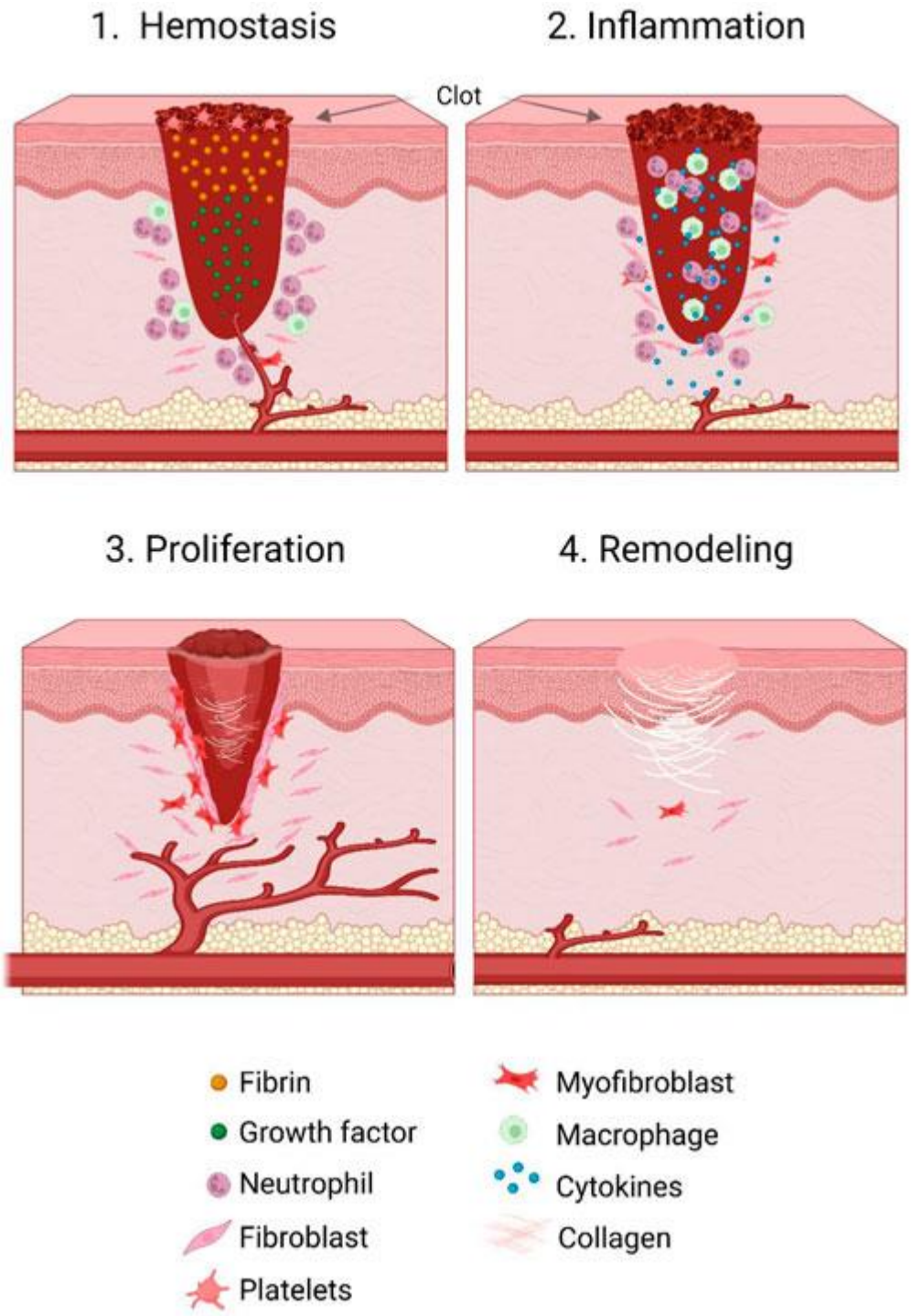

Figure 2: Process of wound healing [19]

- **Hemostasis:** Hemostasis, the initial stage, starts as soon as the damage happens (usually within a few minutes), changing the tissue's integrity. At this point, platelets become active and send signals to help form blood clots (which are made up of fibronectin, fibrin, vitronectin, and thrombospondin) and encourage platelets to form a plug. To further start the healing process, growth factors (chemokines, platelet-

derived growth factor, transforming growth factor-β, and epidermal growth) are produced.

- **Inflamation**: After hemostasis is reached, the immune system enters an inflammatory phase, some immune cells start to lessen the damage, and an immunological barrier against microbes is formed. Leukocytes, particularly neutrophils, are drawn to the site of damage during this phase in order to eradicate germs and foreign debris; as part of the inflammatory response, neutrophils release proinflammatory cytokines, which encourage the production of adhesion molecules. Simultaneously, monocytes go into the wound site and undergo differentiation into macrophages, which have the ability to attract more monocytes and enhance their response.

- **Proliferation**: Reducing the lesioned tissue area is the goal of the proliferative phase, which lasts a few days to weeks. The production of granulation tissue, angiogenesis, collagen deposition, and epidermal regeneration are the characteristics of this phase. Collagen is produced to give the tissue strength after the activated fibroblast first migrates to the wound and produces extracellular matrix proteins (hyaluronan, fibronectin, and proteoglycan) to replace fibrin clots. This granulation tissue, or connective tissue (predominantly type 3 collagens), acts as a scaffold to support the production of new extracellular matrix tissue that is added to the blood artery network by angiogenesis, which is mediated by endothelial cells.

Concurrently, cytokines induce re-epithelialization, wherein proliferating epithelial cells, known as keratinocytes, travel to the wound site to establish a fresh epidermal barrier. Additionally, during this phase, fibroblasts develop into myofibroblasts, which reduce proliferation and increase collagen synthesis, resulting in the constriction of the wound and a reduction in its size.

A normal or acute wound heals according to the above-described process. A chronic wound, on the other hand, results from immune system dysregulation during the healing process; in this case, there is no orderly repair process, it can last longer than three months, and it is not recovered completely. Infections and microbiological films remain in chronic wounds; these wounds are linked to aging, venous ulcers, high blood pressure, obesity, and diabetes. [20]

1.2.3. Topically applied drugs for wound healing

- **Povidone-Iodine 10%:** Povidone-iodine has a quick antibacterial effect that kills a range of bacterial strains in 20 to 30 seconds. Since organic material inactivates iodine, it is recommended to remove dirt and debris before applying povidone-iodine.

- **Chlorhexidine Gluconate and Chlorhexidine Diacetate 2%:** In Healthcare industry, one of the most widely used antiseptics is chlorhexidine. This biguanide antiseptic is positively charged and works against germs by reacting with their negative cell surface membrane to cause disruption, which culminates in their death. It has a long-lasting residual impact together with a broad antibacterial range.

- **Dakin's Solution:** Bleach, commonly known as sodium hypochlorite or Dakin's solution, comes in a range of concentrations, from 0.5% at maximum strength to 0.0125%. Sodium hypochlorite works against germs by releasing chlorine into the surrounding tissues.

- **Tris–Ethylenediaminetetraacetic Acid:** By increasing the permeability of microbial cell membranes, the combination of Tris buffer (tris[hydroxymethyl]aminomethane) and disodium calcium salt of ethylenediaminetetraacetic acid (EDTA) causes microbial mortality when applied topically, especially to gram-negative bacteria.

- **Triple Antibiotic Ointment:** Triple antibiotic ointment is one of the traditional topical antimicrobials used on people and animals. It is made up of three distinct antibiotics: bacitracin, polymyxin B, and neomycin. Although triple antibiotic ointment offers a broad range of antibacterial activity, it is not effective against Pseudomonas species. Triple antibiotic ointment helps patients heal wounds more quickly, have less colonizing microorganisms, and leave fewer scars behind.

- **Octenidine Wound Gel:** Developed as an antiseptic agent in the late 1980s, octenidine dihydrochloride is a cationic surfactant and derivative of pyridine. Gram-positive and gram-negative bacteria, as well as fungi, are all included in its wide antibacterial spectrum. Its action on the skin is protracted, and reports indicate that it remains active for up to 24 hours following application.[21]

- **Nanocrystalline silver dressings**: These dressings consist of an elemental silver-embedded urethane film that releases silver into the wound over time. Depending on the amount of exudate, it has longer-lasting qualities and higher antibacterial action than other silver formulations, which allows dressing changes to occur once a week. Certain nanocrystalline silver dressings, like Acticoat, need to be moistened with water on a regular basis in order to stay activated.[22]

1.3. PHYTO-CONSTITUENTS WITH WOUND HEALING PROPERTY:

Since ancient times, traditional medicine has used herbal remedies to hasten the healing of wounds. Traditional wound care has made use of a wide range of plants and their preparations, particularly because of their enormous capacity to influence wound healing. Through a number of methods, plant-based extracts and/or isolates promote tissue regeneration; these mechanisms frequently combine to enhance the healing process as a whole. Many studies on the topic of managing and treating wounds with plant-derived medications have been conducted recently. Few of the phytocontituents used for the wound healing are listed below:

- **Achillea Millefolium:**

Yarrow, or Achillea millefolium L., is a significant species in the Asteraceae family. It is widely used in traditional medicine throughout multiple cultures, from Europe to Asia, to treat a range of conditions, such as cuts, wounds, abrasions, and diabetic ulcers. Monoterpenes are the most typical metabolites found in the volatile oil isolated from Achillea flowers. Active ingredients isolated from A. millefolium demonstrated antioxidant and anti-inflammatory properties in several in vitro and in vivo tests; these properties were mostly attributable to the presence of flavonoids.

- **Aloe Vera:**

Aloe vera L., also known as Aloe barbadensis Miller, is a perennial herb belonging to the Xanthorrhoeaceae family. It has tubular, bright yellow flower heads. Applications for the mucilaginous gel in pharmaceuticals and beauty products are well-established. This herb has been used to treat a variety of skin issues, including wound healing, rejuvenation, and other dermatological diseases like burns and inflammatory processes. In fact, despite being used extensively as a folk treatment, scientific research on its physiological role in wound healing has just lately been carried out extensively.

Polysaccharides including glucomannan, acetylated polymannan, acemannan, and mannose-6-phosphate, in addition to flavonoids like aloin and emodin, seem to aid in wound healing. According to certain research, acemannan appears to increase bactericidal activity, keratinocyte growth factor-1 (KGF-1) expression, cell proliferation, and vascular endothelial growth factor (VEGF), a molecule crucial for the development of new blood vessels. It also appears to stimulate macrophages.

- **Bletilla Striata:**

As a member of the Orchidaceae family, Bletilla striata has been used for more than 1500 years in Traditional Chinese Medicine to treat mucosal injury to the alimentary canal, wound healing, chapped skin, ulcers, bleeding, bruising, and burns. Pharmacology studies indicate that the plant possesses a wide range of biological activities, including as immune regulatory, anti-inflammatory, and antioxidant properties. Additionally, Bletilla striata has a number of polysaccharides that have been shown to be the main active ingredients in its dried tubers and that have antiviral, antibacterial, anti-aging, and antioxidative properties. [23]

- **Gallic Acid:**

The polyphenolic molecule gallic acid is generated from plants and possesses a broad spectrum of biological and therapeutic properties, such as anti-inflammatory, antioxidant, anti-microbial, anti-cancer, and wound healing properties. In the control of internal hemorrhages, it is also employed as an astringent. Research has shown that Gallic acid has potent antioxidant properties that directly increase the expression of genes related to antioxidant defenses. Additionally, it has been shown that under both normal and hyperglycemic conditions, Gallic acid accelerates the migration of keratinocytes and fibroblasts, which activates growth factors like c-Jun N-terminal kinases (JNK), focal adhesion kinases (FAK), and extracellular signal-regulated kinases (Erk) that are involved in wound healing.

- **Quercetin**

A flavonoid compound, Quercetin which is found in most of the herbs, vegetables and fruits Quercetin is reported to have the powerful anti-inflammatory, anticancer, and antioxidant supplements. Quercetin is also effective in wound healing by increasing the production of

collagen and fibronectin. Quercetin may also help speed wound healing; studies have also shown that quercetin helps repair damage to nerve tissues in skin wounds. Quercetin incorporated collagenous matrix treated animal showed a better healing with an increase in proliferation of cells and wound contraction than the control group. [24]

- **Curcumin**

One of the numerous species in the Curcuma genus, curcumin (Curcuma longa) is a perennial, herbaceous, rhizomatous plant that is a member of the Zingiberacee family. The spice, which is derived from the rhizome of Curcuma longa, also known as "turmeric," has antioxidant polyphenolic components. Curcumin has long been utilized in Ayurvedic and folk medicine to treat a wide range of inflammatory conditions. Its anti-inflammatory properties derive from its capacity to reduce histamine synthesis and extend the effects of cortisol, an anti-inflammatory adrenal hormone that is produced naturally.

One of the three curcuminoids found in turmeric is curcumin, which is a very pleiotropic substance in nature. It has been thoroughly investigated recently as an anti-aging, antiviral, antibacterial, and wound-healing agent. Curcumin has the ability to heal wounds because of its anti-inflammatory, antioxidant, and radical-scavenging properties. All phases of wound healing are affected by curcumin. Curcumin has been demonstrated to block NF-kB activity throughout the inflammatory stage as well as the synthesis of TNF-alpha and IL-1.

Curcumin has shown to give keratinocytes and fibroblasts the best resistance against hydrogen peroxide in in vitro experiments. Curcumin promotes fibroblast migration, granulation tissue development, collagen deposition, and re-epithelialization during the proliferative stage.

Curcumin increases TGFbeta synthesis and fibroblast proliferation, which enhances wound contraction during the remodelling period. Another way to inhibit both acute and chronic inflammation is to prevent the synthesis of the enzymes lipoxygenases, cyclooxygenases, and inducible nitric oxide synthase. [23]

CHAPTER 2:

LITERATURE SURVEY

2. REVIEW OF LITERATURE

1. Sodium alginate (SA) and HPMC composite wafers and films were created for nicotine (NIC) replacement therapy administered orally. Several concentration ratios of magnesium aluminium silicate (MAS) were added to NIC in order to stabilize its mechanical characteristics.Investigations were conducted on the formulations' internal and external morphology, physical form, thermal characteristics, swelling, mucoadhesion, drug content, and release behavior. The composite formulations' physico-mechanical characteristics were altered by MAS, which resulted in a decrease in mechanical hardness, collapsed wafer pores, increased film surface roughness, increased crystallinity, and decreased wafer mucoadhesion. MAS, on the other hand, enhanced drug-loading capacity by increasing swelling in films and wafers as well as the interaction between NIC and SA. Furthermore, NIC was released from wafers and films at different rates as a result of MAS. According to the findings, MAS 0.25 was the best formulation for stabilizing NIC in the composite formulations.[25]

2. Wafers that have been lyophilized may be used as drug delivery vehicles for open wounds. Two types of wafers were created: one using low molecular weight sodium alginate (SA) and the other using xanthan gum (XG), both modified with high molecular weight methylcellulose (MC). We looked at these wafers' swelling and flow characteristics on suppurating surface models both qualitatively and quantitatively. The wafers stuck to the surfaces right away, absorbing water to change from glassy, porous solids to extremely viscous gels. There were distinct differences in the behavior of the SA and XG systems, and the rate at which this happened varied for the series under study. There was a clear correlation between the flow rate and MC content for SA wafers. The rate at which the SA wafers flowed across a model gelatine surface was lowered by increasing the amount of MC. The impact of higher MC content on both wafer series was measured using flow rheometry, which for the SA series revealed a marked rise in apparent viscosity as a function of MC content increments. These outcomes were consistent with the gelatine model. The yield stress typical of xanthan gels was shown to be responsible for the reluctance of an unmodified, swollen XG wafer to flow in contrast to the relative ease of an unmodified, low molecular weight SA. Through the connection of helical backbone

structures, XG is known to display intricate, loosely coupled network topologies in solution. The potential of lyophilized wafers as practical drug delivery devices for suppurating wounds was underlined by the addition of sodium fluorescein as a visible model for a soluble medication. [26]

3. Wafers that have been lyophilized are being developed as topical drug delivery devices to treat chronic wounds. This work reports the synthesis of xanthan wafers that include a non-ionic surfactant and a selective, insoluble MMP-3 inhibitor (UK-370,106). The purpose of the wafers is to deliver precise dosages of UK-370,106 to a suppurating wound bed. The investigation of UK-370,106's stability in the wafer was conducted by a mix of thermal, light scattering, and microscopic techniques, in comparison to a non-lyophilized gel suspension. During an accelerated stability trial (12 weeks, 40 ◦C), the particle size distributions in wafers loaded with UK-370,106 remained stable, whereas the mean particle size in a non-lyophilised solution grew by 15 m during the same time frame. Wafers loaded with UK-370,106 were subjected to thermal analysis, which revealed an unanticipated interaction between the drug and the surfactant. This interaction was then explored using basic mixes of each component. It was determined that UK-370,106 and the non-ionic surfactant can create an in situ solvate, and that this could have an impact on UK-370,106's stability throughout the formulation process. Additional worries about the wafer's high water content (14%), which could have affected the stability of the product, were unfounded, and it was determined that these innovative delivery methods offered a good substitute for gel suspensions. [27]

4. The aging population is expected to have a significant impact in the ensuing decades because of lower birth rates and longer life expectancies. Because they may have more medical issues that make swallowing prescription medications difficult, such as dysphagia, older persons typically need more prescription medications. In order to prevent thrombosis in older patients with dysphagia, this study aims to design, characterize, and optimize composite wafers for possible oral and buccal delivery of low dose aspirin. In order to determine the best polymer combinations, combinations of metolose (MET) with carrageenan (CAR) and MET with low molecular weight

chitosan (CS) were first dissolved in water in varied weight ratios to create blank (BLK) wafers (no loaded medication). On the other hand, 45% v/v ethanol was used to create drug-loaded (DL) wafers, which helped fully solubilize the aspirin. Texture analyzers (hardness, mucoadhesion), scanning electron microscopy (SEM), X-ray diffractometry (XRD), differential scanning calorimetry (DSC), attenuated total reflectance – Fourier transform infrared (ATR-FTIR), thermogravimetric analyzer (TGA), and swelling capacity were used to characterize the formulations. In addition to relying on the ratios of the polymers utilized, wafers with higher total polymer concentration were also more resistant to penetration (MET:CAR 1:1 samples B2, C2), MET:CS 1:1 (sample E2), and MET:CS 3:1 (sample F2). Samples C2, B2, E2, and F2 displayed the best qualities based on the characterisation. XRD revealed that the DL wafers were crystalline because of the aspirin content, but the BLK wafers were amorphous. While the DL wafers had a more compact polymeric matrix with aspirin scattered across the surface, the SEM analysis of the BLK wafers verified the existence of holes within the polymer matrix. The DL wafers had better swelling capacity and adhesion values with phosphate buffer saline (PBS) than with simulated saliva (SS), and they also demonstrated the good flexibility needed for patient handling and transportation. According to research on drug breakdown, aspirin was released quickly in the first 20 minutes and then constantly throughout the next hour. The broad peak between 2500 and 3300 cm−1 and peak changes around 1750 cm−1 indicated by FTIR verified aspirin's interaction with the polymers. For the delivery of low dose aspirin to elderly patients with dysphagia, lyophilized CAR: CS 1:3 (sample DL13), MET:CS 1:3 (sample DL8), and MET:CAR 3:1 (sample DL1) wafers appear to be a highly promising approach. [28]

5. Chitosan lyophilized wafers have been created as possible vehicles for protein drug delivery via the buccal mucosa. Aqueous gels of the polymer with different amounts of d-mannitol as a cryoprotectant and glycerol as a plasticizer were lyophilized to create wafers. To determine which formulation was best for additional development, the various formulations were evaluated based on their physico-mechanical characteristics. Bovine serum albumin was added to the optimized formulation, which contained 6.5 mg of plasticizer and cryoprotectant each. It was then lyophilized with or without annealing. By analyzing thermal events prior to lyophilization and

potential phase separation of bovine serum albumin following lyophilization, differential scanning calorimetry was utilized to establish the proper lyophilization cycle. The tensile mode texture analysis was used to study the in vitro mucoadhesive qualities; thermogravimetric analysis was used to determine the residual moisture content; and 0.1 M phosphate buffered saline was used for investigations on medication release and hydration capacity. X-ray diffractometry and scanning electron microscopy were used, respectively, to investigate the microscopic architecture and crystallinity. The annealing method affected the BSA release, microscopic architecture, ease of hydration, and in vitro mucoadhesive properties. For the annealed and non-annealed wafers, a cumulative percentage drug release over 7 hours was found to be 91.5% and 80.1%, respectively. The outcomes demonstrated the potential of using lyophilized chitosan wafers to deliver protein-based medications to the buccal mucosa. [29]

6. Using ethyl cellulose (EC), hydroxypropyl methylcellulose (HPMC), and polyvinyl pyrrolidone (PVP) as a film forming, transdermal wafers of the Glibenclamide (GBE) were created. The impact of a binary combination of penetration enhancer and polymer on physicochemical characteristics such as drug content, thickness, weight variation, and in vitro permeation was assessed. Rat abdomen skin was used as a penetration barrier in an in vitro skin penetration research for the binary mixtures in the Franz diffusion cell. The combinations of EC/HPMC (8.5:1.5) and EC/PVP (3:2) demonstrated good permeability. The permeability is further increased by adding a penetration enhancer to the binary combination. [30]

7. There are numerous bandages available for the healing of chronic wounds, however they frequently fall short of the desired outcomes. The current study suggests the manufacture of a novel dressing, lyophilized liposomal wafers with improved wound healing capability, to address some of their shortcomings. Gatifloxacin (GTX), a fourth-generation fluoroquinolone antibiotic with in vitro action against both Gram-positive and Gram-negative bacteria, is the medication included in the formulation. The formulation was created in three steps: first, liposomes were made; next, chitosan was used to turn the liposomes into a gel; and finally, this gel was lyophilized to

create liposomal wafers. Transmission electron microscopy (TEM), scanning electron microscopy (SEM), in vitro cumulative release, particle size, entrapment efficiency, and other tests were performed on liposomes that were created by adjusting the concentration of lipid and cholesterol. Using chitosan, liposomes were transformed into liposomal gel, which was then assessed for spreadibility, texture, clarity, viscosity, and in vitro drug release. In order to create liposomal wafers, this liposomal batch was then lyophilized. It was then put through drug release experiments, SEM, differential scanning calorimetry, and X-ray diffraction. The in vivo experiments were conducted on Wistar rats, and histological analysis was used to establish the wafers' capacity to cure wounds. [31]

8. An antiviral medication called acyclovir is commonly recommended to treat the herpes virus. Nevertheless, because of the medication's low absorption (10–26.7%), frequent administration is necessary. The goal of the current study was to create a self-dissolving microneedle system that would deliver acyclovir both locally and systemically by applying a topical lyophilized wafer to skin that had received microneedle treatment and delivering the medication to the infection site. Extracted rat skin was pierced by microneedles made with hydroxypropyl methylcellulose (HPMC) (8% w/w) or HPMC (8% w/w)-polyvinyl pyrrolidone (PVP) (30% w/w), demonstrating adequate mechanical strength and quick polymer breakdown. Acyclovir (40% w/w; 200 mg of medication) was combined with 10% w/w gelatin, 5% w/w mannitol, and 5% w/w sodium chloride to create the topical wafer. The amorphous form of acyclovir was uniformly distributed across the wafer, as verified by thermogravimetric analysis (TGA) and differential scanning calorimetry (DSC). Fourier transform infrared spectroscopy (FTIR) study of the lyophilized wafer revealed no evidence of polymer–drug interaction. Scanning electron microscopy (SEM) research revealed that the wafer had a sufficiently porous structure for fast hydration. The skin was pre-treated with a self-dissolving microneedle array for five minutes prior to ex-vivo examination, and the wafer was then placed on the microporated skin. The topical wafer yielded a skin concentration that was approximately 7–11 times higher than the ID99, but with a shorter lag-time. Around 2.58 µg/ml of Cmax was attained in rabbit plasma during the course of a 24-hour investigation, according to in-vivo testing. Based on our research, it appears that the

self-dissolving topical wafer, which was previously suggested, could effectively treat systemic infections as well as those that reside in the skin layer. [32]

9. To promote chronic wound healing, wafers containing sodium alginate (50/50) or Polyox with carrageenan (75/25) at weight ratios of streptomycin and diclofenac were created. Using a lyophilization cycle that included an annealing phase, gels were freeze-dried. Wafers were evaluated for their shape, mechanical properties, and in vitro functional properties (adhesion, swelling, and drug release in the presence of wound fluid simulation). Both the drug-loaded (DL) and blank (BLK) wafers had a non-brittle nature and were smooth, supple, and beautiful in appearance. Wafers' improved porosity was aided by annealing, although this process was impacted by drug addition. The mechanical analysis revealed that the wafers were both flexible and strong enough to sustain typical loads without causing harm to the skin's freshly produced tissue. Differences in pore size and sodium sulfate generated as a result of the two medications' salt forms may be the source of variations in swelling, adhesion, and drug release properties. DL wafers demonstrated regulated release of diclofenac and streptomycin, but BLK wafers had comparatively increased adherence and edema. Due of diclofenac's anti-inflammatory properties, the optimized dressing may assist to lessen bacterial infection and may also hasten wound healing by reducing swelling and pain associated with injury. [33]

10. In order to create medicated wafer dressings that may be used on chronic wounds, two bioactive polysaccharide polymers—kappa-carrageenan (CARR) and sodium alginate (SA)—were combined with microbial biosurfactants (BSs) in this study. Using textural analysis (mechanical strength and in vitro wound adhesion), attenuated total reflectance, and scanning electron microscopy (SEM), wafers were loaded with BSs at concentrations of 0.1% and 0.2% rhamnolipids (RL) and 0.1% and 5% sophorolipids (SL). Exudate handling properties (pore analysis, swelling index, water absorption (Aw), equilibrium water content (EWC), evaporative water loss (EWL), and water vapor transmission rate (WVTR), as well as Fourier transform infrared (ATR-FTIR) spectroscopy and X-ray diffraction (XRD). With a hardness range of 2.7–4.1 N, the wafers had a tactile and ductile look. They can tolerate typical stresses

while remaining flexible to protect the developing skin tissues. The wafers' pore diameters ranged from 78.8 to 141 μm, and there were no apparent BSs on the surface or pore walls. The wafers were porous (SEM). The wafers' porosity was increased by the BSs to levels over 98%, whilst the Aw and EWC had corresponding ranges of 2699–3569% and 96.58–98.00%. After 24 hours, the EWL varied between 85 and 86%, while the WVTR varied between 2702 and 3080 g/m2 day−1. Seven distinctive functional groupings that were reliably communicated in the ATR-FTIR spectra demonstrated the compatibility of BSs within the CARR-SA matrix. These cutting-edge medicated dressing prototypes may contribute to quicker wound healing. [34]

11. Because of unprotected heterosexual vaginal sex as well as other social and economic disadvantages, women are particularly vulnerable to acquired immunodeficiency syndrome (AIDS) and other sexually transmitted diseases (STDs). Our goal was to create and refine abacavir's vaginal film, a powerful nucleoside reverse transcriptase inhibitor, for use in the management of HIV and AIDS. Sodium alginate (Na-alginate) was the primary polymer, copolymer Hydroxypropyl Methylcellulose E 15 (HPMC E 15), and humectant glycerol were used in the solvent evaporation process to make abacavir films. Here, abacavir sulphate (ABC) was the medication. The tensile strength, percentage of elongation at break, swelling capacity, drug content (mg/cm2), thickness, folding endurance, bioadhesion, pH, moisture content, and SEM were among the physicochemical characteristics for which films were tuned. With FTIR Spectra, the drug-polymer interaction was investigated. The dissolution device was used to complete the drug release investigation. A study in vivo was also conducted. This recently developed film can be viewed as a unique medication carrier system for the treatment of AIDS and other STDs. It is one sort of sustain release film. It was appropriate for both systemic and local effects. The films have strong physical and chemical qualities as well as strong visual appeal. [35]

12. Hydrogels were lyophilized to create calcium alginate (CA) wafer dressings, which allowed ciprofloxacin (CIP) to be applied directly to the site of infection on diabetic foot ulcers (DFUs). Scanning electron microscopy (SEM), texture analysis (for

mechanical and in vitro adhesion qualities), X-ray diffraction (XRD), and Fourier transform infrared spectroscopy (FTIR) were used to physically evaluate the dressings. Additionally, functional characteristics that are necessary for wound healing were examined, including moisture content, antimicrobial activity, in vitro drug release and kinetics, water absorption (Aw), equilibrium water content (EWC), water vapor transmission rate (WVTR), porosity, and cell viability (MTT assay). The wafers had a consistent thickness and texture, were malleable, and were soft in nature. Wafers' high porosity allowed them to exhibit the best fluid-handling qualities as a wound dressing (SEM). The dressings' crystalline nature was verified by XRD, and hydrogen bond formation between CA and CIP was revealed by FTIR. The dressings demonstrated rapid drug release at first, followed by prolonged drug release. This can block and stop both Gram-positive and Gram-negative bacteria from causing re-infection. Additionally, the dressings demonstrated biocompatibility with human adult keratinocytes (> 85% cell viability over 72 hours). It will therefore be a potential medicated bandage for patients, whose DFUs are afflicted with germs that are resistant to drugs. [36]

CHAPTER 3

AIM AND OBJECTIVES

3. AIM AND OBJECTIVE:

Aim: The aim of the present work is to formulate and evaluate a curcumin loaded lyophilized wafer that can be used for wound healing process.

Following are the main objective of the current work:

- Pre-formulation study of drug.
- Preparation of drug loaded lyophilized wafer.
- Characterization of lyophilized wafer.
- Determination of Release kinetics of the drug.
- Anti-microbial study of the drug was determined used disc diffusion method.

CHAPTER 4:

MATERIALS AND REAGENTS

4. MATERIALS AND REAGENT:

Drugs and Reagents:	**Dealers:**
Pure curcumin	Yarrow Pharma Ltd.
HPMC K 15M	Yarrow Pharma Ltd.
Ethyl Cellulose	CDH (P) Ltd.
Polyvinylpyrrolidone(K-30)	Sisco Research Laboratories Pvt Ltd.
Denatured Ethanol	Changshu Song Sheng Fine Chemical
Chloroform	Merck Life Science Pvt. Ltd.
Potassium Dihydrogen Phosphate	Loba Chemie Pvt. Ltd.
Disodium hydrogen phosphate	Loba Chemie Pvt. Ltd.
Sodium Chloride	Qualigens Fine Chemicals

Table 1: shows drugs and reagents used in the present work and their dealers.

4.1. CURCUMIN [37,38,39,40,41,42,43]

Drug Description	Curcumin, also called diferuloylmethane, is an ingredient that is present in both [Curcuma xanthorrhiza oil] and turmeric (Curcuma longa), the golden spice. With antibacterial, anti-inflammatory, hypoglycemic, antioxidant, wound-healing, and antimicrobial properties, it is a very pleiotropic compound. Owing to these characteristics, curcumin has been researched for the therapy and supportive care of clinical disorders such as depression, multiple myeloma, proteinuria, breast cancer, and non-small cell lung cancer (NSCLC).
Drug Class	Anti-Inflammatory Agents, Non-Steroidal, Antineoplastic Agents, Enzyme Inhibitors
Molecular Formula	$C_{21}H_{20}O_6$

Chemical Structure	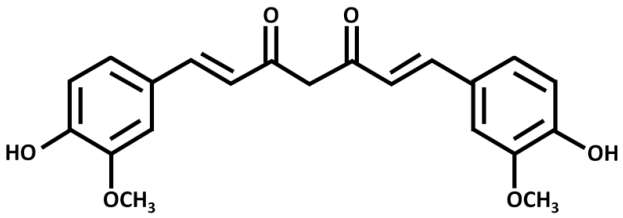
Iupac Name	(1*E*,6*E*)-1,7-bis(4-hydroxy-3-methoxyphenyl)hepta-1,6-diene-3,5-dione
Molecular Weight	368.4 g/mol
Brand Name	Curcumin, Curcuma Longa, Turmeric Root, and Wild Curcuma.
Melting Point	183ºC
Route Of Administration	Curcumin can be administered orally, intraperitoneally , intravenous (IV) injection, nasally, topically and subcutaneously,
Half Life	6-7 hours
Mechanism Of Action	By interacting with NF-κB, curcumin reduces the inflammatory response of TNF-α-stimulated human endothelial cells, hence exhibiting anti-inflammatory properties. Moreover, curcumin has the ability to inhibit platelet-derived growth factor (PDGF).
Adverse Effect	May cause skin irritation. Causes serious eye irritation. May cause respiratory irritation.

Drug-Drug Interactions	Agmatine, Quinacrine, Benzyl alcohol, Bupropion

4.2. HPMC K 15M [44,45,46,47]

Description	Hydroxypropyl methylcellulose (HPMC) is a member of the class of cellulose ethers in which one or more of the three hydroxyl groups found in the cellulose ring have been substituted for hydroxyl groups. Hydrophilic (water soluble), biodegradable, and biocompatible, HPMC is a polymer with several uses in medicine delivery, cosmetics, adhesives, coatings, textiles, dyes and paints, and agriculture. It is also possible to employ both aqueous and nonaqueous solvents with HPMC because it is soluble in polar organic solvents. Its solubility in both hot and cold organic solvents gives it remarkable features.
Molecular Formula	$C_{56}H_{108}O_{30}$
Chemical Structure	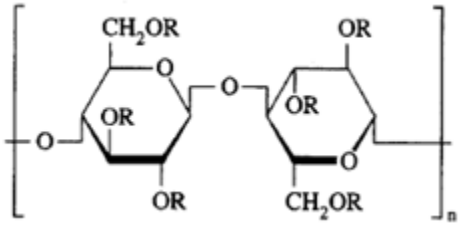
IUPAC Name	(2*R*,3*R*,4*S*,5*R*,6*R*)-2,3,4-trimethoxy-6-(methoxymethyl)-5-[(2*S*,3*R*,4*S*,5*R*,6*R*)-3,4,5-trimethoxy-6-(methoxymethyl)oxan-2-yl]oxyoxane;1-[[(2*R*,3*R*,4*S*,5*R*,6*S*)-3,4,5-tris(2-hydroxypropoxy)-6-[(2*R*,3*R*,4*S*,5*R*,6*R*)-4,5,6-tris(2-hydroxypropoxy)-2-(2-

	hydroxypropoxymethyl)oxan-3-yl]oxyoxan-2-yl]methoxy]propan-2-ol
Molecular Weight	1261.4 g/mol
Brand Name	Hypromellose; Celacol HPM 5000
Melting Point	225-230ºC
Solubility	Both aqueous and nonaqueous solvents can be used with HPMC because it is soluble in polar organic solvents. Its solubility in both hot and cold organic solvents gives it remarkable features.

4.3. ETHYL CELLULOSE:[48,49,50]

Description	In many different types of Pharmaceutical Products, ethyl cellulose is employed as a film maker, binder, dispersion agent, stabilizer, water retention agent, and controlled release agent.
Molecular Formula	$C_{20}H_{38}O_{11}$

Chemical Structure	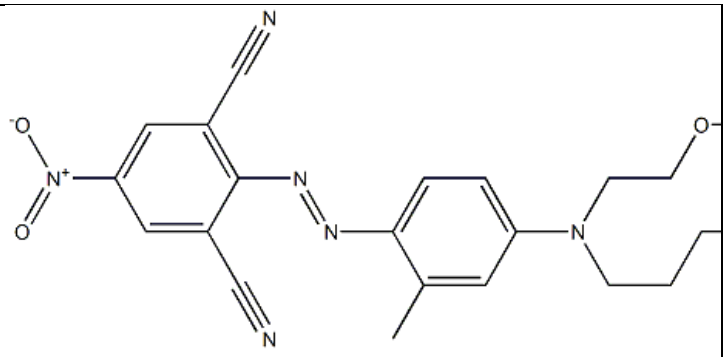
IUPAC Name	2-[4,5-diethoxy-2-(ethoxymethyl)-6-methoxyoxan-3-yl]oxy-6-(hydroxymethyl)-5-methoxyoxane-3,4-diol
Molecular Weight	454.5 g/mol
Melting Point	240-255 °C
Solubility	Ethyl cellulose is practically insoluble in glycerol, propane-1,2-diol, and water. However, depending on the ethoxyl content, it can be soluble in different amounts in a number of organic solvents.

4.4. POLYVINYLPYRROLIDONE (K-30) [51,52,53,54]

Description	PVP K-30, also known as polyvinylpyrrolidone K-30, serves as a film forming and stabilizer, giving a firm and stable grip. This powdered polyvinylpyrrolidone polymer is amorphous, hygroscopic, and has good compatibility with acrylate thickeners. It can be used as a dispersion for hair colorants and as an emulsion stabilizer in creams and lotions. This component dissolves in water and works well with a wide range of resins as well as most inorganic salts.

Molecular Formula	C_6H_9NO
Chemical Structure	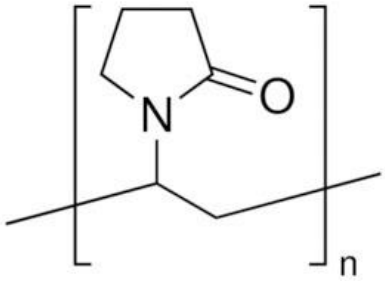
IUPAC Name	1-ethenylpyrrolidin-2-one
Molecular Weight	111.14 g/mol
Melting Point	150ºC-180ºC
Solubility	Soluble in water, ethanol, methanol, chloroform, acids, and amines. Insoluble in ethers, hydrocarbons, some esters, some ketones, and mineral oil.

4.5. DENATURED ETHANOL:[55,56,57]

Description	A hydroxy group replaces one of the hydrogens in ethane, which is the primary alcohol known as ethanol. As an antiseptic, polar solvent, neurotoxin, CNS depressant, teratogenic agent, NMDA receptor antagonist, protein kinase C agonist, disinfectant, human, Saccharomyces cerevisiae, Escherichia coli, and mouse metabolite, among other roles it plays in the body. It belongs to the class of ethanols, is a

	volatile organic chemical, an alkyl alcohol, and a primary alcohol. It is an ethoxide's conjugate acid.
Molecular Formula	CH_3CH_2OH
Chemical Structure	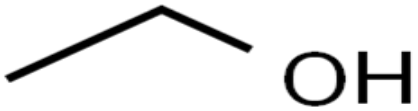
IUPAC Name	Ethyl alcohol
Molecular Weight	46.07 g/mol
Melting Point	-114.1°C
Solubility	Very soluble in water.

4.6. CHLOROFORM:[58,59,60,61]

Description	Chloroform has a mildly sweet taste and a nice, non-irritating smell. Only at extremely high temperatures will it burn. It is colourless. Chloroform is no longer utilized during surgery as an inhalation anaesthetic as it was in the past. Chloroform can be created in small amounts when chlorine is introduced to water, and it is also utilized nowadays to generate other compounds.

Molecular Formula	$CHCl_3$
Chemical Structure	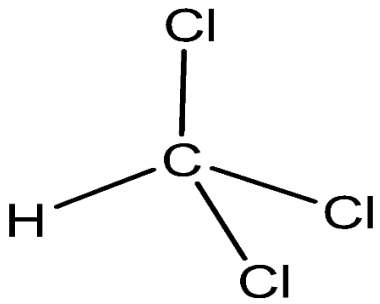
IUPAC Name	Trichloromethane
Molecular Weight	119.37 g/mol
Melting Point	-63.5ºC
Solubility	Soluble in ether and alcohol, but very sparingly soluble in water.

4.7. POTASSIUM DIHYDROGEN PHOSPHATE[62,63,64]

Description	There are several applications for potassium dihydrogen phosphate (KH2PO4), an inorganic salt. Other names for it include potassium biphosphate, potassium phosphate monobasic, and potassium acid phosphate. KH2PO4 is used in applications that concentrate on its nonlinear optical features, as well as in pharmaceutical and other preparations as buffering agents and agricultural plant nutrients.
Molecular Formula	KH_2PO_4

Chemical Structure	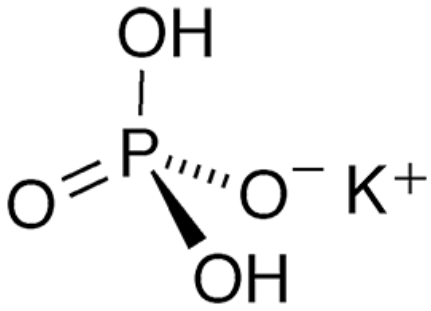
Molecular Weight	136.086 g/mol
Melting Point	252.6 °C
Solubility	Solubility in water (90 ℃ for 83.5g/water). Insoluble in alcohol.

4.8. DISODIUM HYDROGEN PHOSPHATE[65,66,67]

Description	di-Sodium hydrogen phosphate dihydrate is typically used as a buffer component in biomolecule downstream processing and liquid formulation.
Molecular Formula	Na_2HPO_4
Chemical Structure	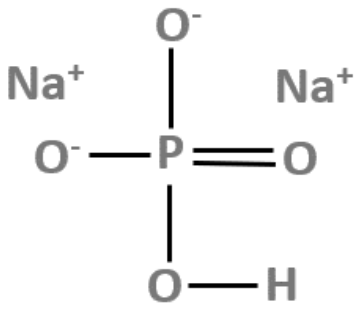
Molecular Weight	141.959 g/mol
Melting Point	250°C

Solubility	Freely soluble in water. Insoluble in ethanol

4.9. SODIUM CHLORIDE :[68,69]

Description	With sodium (1+) serving as the counterion, sodium chloride is an inorganic chloride salt. It performs the functions of an emetic and a flame retardant. It's a salt of inorganic sodium and chloride. It may be used for preparing phosphate buffer 7.4.
Molecular Formula	NaCl
Chemical Structure	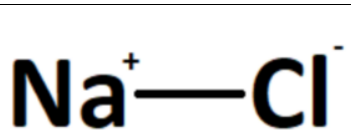
Molecular Weight	58.44 g/mol
Melting Point	801°C
Solubility	Soluble in water but solubility is decreased by hydrogen chloride

Table 2: depicts characteristics of drugs and reagents used for the present work.

CHAPTER 5

METHODS AND CHARACTERIZATON

5.1. PRE-FORMULATION STUDIES

5.1.1. PHYSICAL CHARACTERIZATION:

The physical characterization for colour, texture and odour of the Drug were carried out by visual representation.

5.1.2. DETERMINATION OF MELTING POINT:

Using a Bunsen burner, heat was applied to one end of the capillary tube to seal it. The capillary tube's open end was then used to insert the drug Curcumin. Following the injection of a predetermined dosage into the capillary tube, the tube was gently tapped on the closed end to fill it to a height of one to two millimetres. The capillary tube was inserted into the tube holder of the melting point apparatus (Monarch Scientific Industries) in order to measure the drug's melting point. The temperature control knob was turned to the correct setting. Both the starting temperature at which the medication began to melt and the end temperature at which it melted entirely were measured and recorded. The drug's melting point was ascertained by averaging the two temperatures. The process was carried out three times in order to get an acceptable result.

5.1.3. DETERMINATION OF CALIBERATION CURVE:

- **Preparation of phosphate buffer saline pH 7.4**

  For preparation of pH 7.4 saline solution of phosphate buffer, 2.86g of NaH_2PO_4 and 0.2g of KH2PO4 were combined with distilled water up to 1000 ml. To the mixture, 8 grams of NaCl were added. The pH of the mixture was brought to 7.4 by adding an appropriate buffer component after it was agitated with a stirrer. [70]

- **Preparation of standard solution**

  After precisely weighing 10 mg of curcumin, it was added to a 100 ml volumetric flask. The volumetric flask was completely filled with a 1:1 mixture of phosphate buffer (pH 7.4) and ethanol. A clear standard stock solution was produced. 100 ppm solution was prepared

- **Determination of maximum wavelength**

  A solution containing 10 µg/ml of curcumin was scanned in a UV-visible spectrophotometer between 200 and 800 nm in wavelength. The blank was a combination of ethanol (1:1) and pH 7.4 phosphate buffer.

- **Preparation of standard calibration curve**

  The absorbance of a curcumin solution in the concentration range of 2–20 µg/ml, which was generated from stock solution (100 ppm) in 1:1 phosphate buffer (pH 7.4) and ethanol mixture, was measured in triplicate at 429 nm to obtain the standard calibration curve for curcumin. The curcumin calibration curve was then drawn on an x-axis representing curcumin concentration in ppm and y-axis representing absorbance. [71]

5.2. FABRICATION OF LYOPHILIZED WAFER

A mixture containing a particular amount of HPMC, EC and PVP K30 at a distinct proportion of ((5:1:0.5 w/w; (amount wise 961.32, 192.26 and 96.12 mg)) respectively were added in a solvent mixture of chloroform and ethyl alcohol in 1:1 ratio, and stirred with the help of a Magnetic Stirrer (REMI 2MLH) at a speed of 600 rpm., to form a viscous and transparent liquid. [72] Four different batches of lyophilized wafer were formulated with drug amounts 50mg, 100mg, 150mg and without drug and labelled as F1, F2, F3 and Blank respectively. These different amounts of the drug (curcumin) were thereafter added to the transparent polymeric solution and further stirred on a magnetic stirrer till the curcumin was dissolved until a bright yellow homogeneous solution was found.

A cylindrical glass mould of inner diameter 3 inches was taking and one end of it was attached by the backing layer (130 cm^2, SCOTCHPAK TAN EXCO FILM 1109) the drug-carrier polymeric mixture was then poured carefully inside the glass mould, over the backing layer stuck on one end. The other end of the cylindrical apparatus was then covered with aluminium foil wrap and made tiny holes with a 21 gauge needle (DISPO VAN single use hypodermic needles) for air to pass during lyophilizer. The glass apparatus was then carefully placed inside the vacuum chamber of the lyophilizer and lyophilized for 5 hours. The lyophilized wafer was formed and then pealed from the cylindrical glass wall with the help of

a fresh blade. The wafers thus produced with different concentrations of Curcumin were then stored in different zipper pouches to avoid contamination.

Ingredients	**Blank**	**F1**	**F2**	**F3**
HPMC(mg)	96.12	96.12	96.12	96.12
Ethyl Cellulose(mg)	192.26	192.26	192.26	192.26
Polyvinyl pyrrolidone(mg)	961.32	961.32	961.32	961.32
Ethyl alcohol(ml)	5	5	5	5
Chloroform(ml)	5	5	5	5
Curcumin(mg)	--	50	100	150

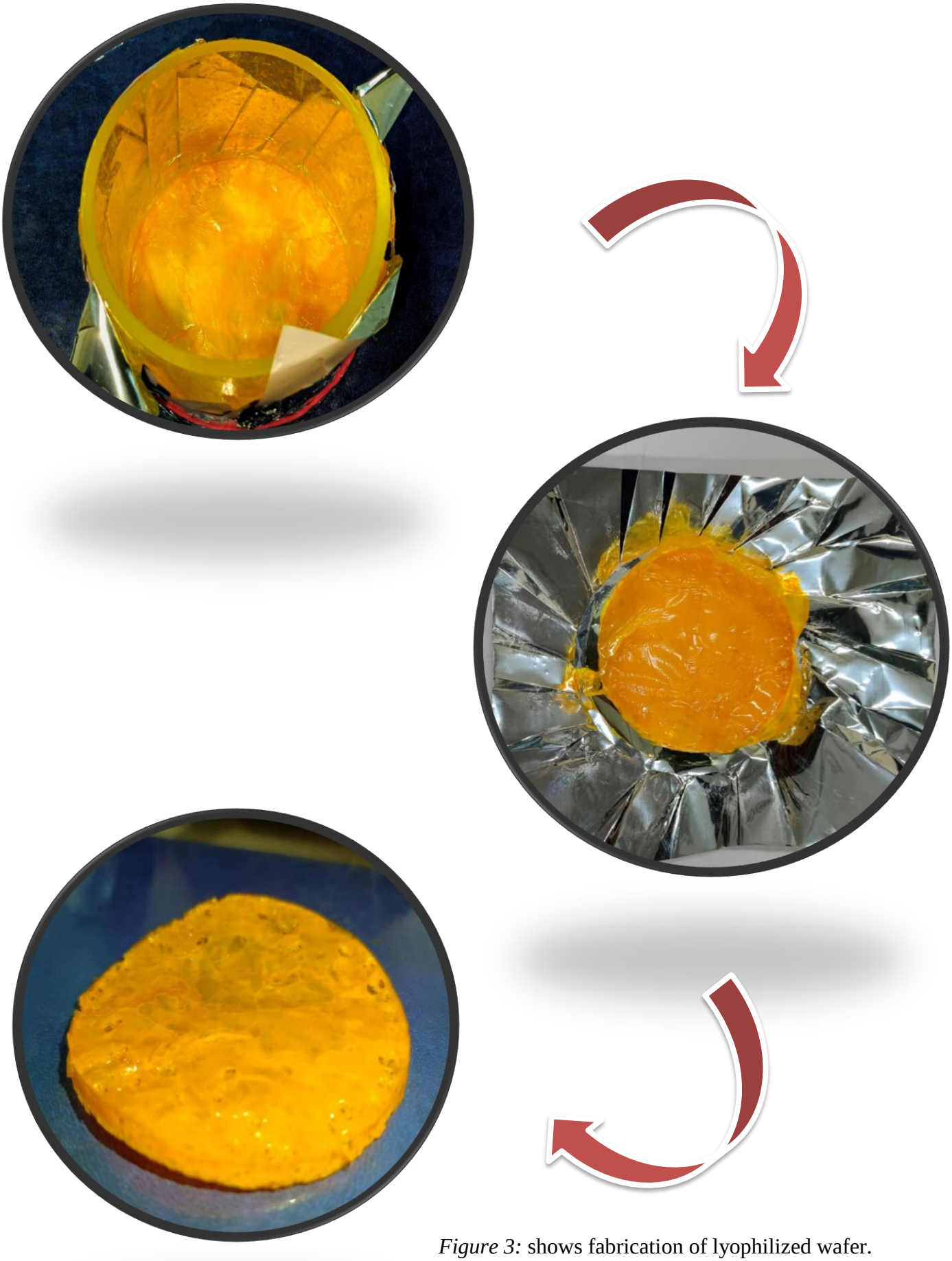

Figure 3: shows fabrication of lyophilized wafer.

5.3. CHARACTERIZATION:

5.3.1. THICKNESS:

Thickness of the wafers were determined using a digital Vernier Caliber. The thickness of each wafer was taken at four different places around the wafer.

5.3.2. DENSITY:

The density of the lyophilized wafers were determined by first noting the average mass of the samples and their volume. The data was then put into the formula:

$$\boldsymbol{Density = \frac{Mass}{Volume}}$$

5.3.3. FOLDING ENDURANCE:

The entire wafer was utilized to evaluate the film's folding endurance. The wafer was repeatedly folded at the same location both horizontally and longitudinally, until it broke, to determine the folding endurance. The value of folding endurance is determined by the number of times the film could be folded in the same way without breaking. A total number of folding times has been measured and documented. [73]

5.3.4. PERCENTAGE YIELD:

By weighing the actual wafers and the chemicals used in their preparation—that is, the weight of HPMC, polyvinyl pyrrolidone, and ethyl cellulose—the percentage yield of lyophilized wafers was determined. The following formula was used to compute the percentage yield [74]:

$$\%\boldsymbol{yield\ of\ Wafer} = \left\{\frac{\boldsymbol{Actual\ weight\ of\ the\ lyophilized\ wafer}}{\boldsymbol{Weight\ of\ HPMC + PVP + Ethyl\ Cellulose}}\right\} * \mathbf{100}$$

5.3.5. TENSILE STRENGTH:

The tensile strength of the lyophilized wafers were calculated using a texture analyzer (TA.XT plus, Stable Micro Systems, UK). The samples with a length of 5 cm and a width of 2 cm were set in the tensile grip of the instrument. The sample was stretched with an upper movable button by applying a triggering force of 5 g, and the force required to tear the wafer

into two parts was calculated. The other instrumental parameters/details have been mentioned in the individual figures/results.

5.3.6. SWELLING INDEX (%) DETERMINATION:

Wafers were attached to a perforated backing membrane, and each formulation was submerged in 15 millilitres of phosphate buffered saline (pH 7.4) to evaluate the wafers' swelling capacities. Weight changes were tracked over periods of 70, 80 and 90 minutes. The wafer was carefully taken out for each time span, tapped with tissue paper to remove any excess water, and then weighed using a weighing balance. [75] For every sample, three duplicates were made, and the following equation was used to compute the swelling index (%):

$$\boldsymbol{Swelling\ index} = \frac{\boldsymbol{Ws - Wd}}{\boldsymbol{Wd}} \boldsymbol{X100}$$

Where,

Wd = dry weight of film or wafer,

Ws = weight of film or wafer after swelling.

5.3.7. WATER VAPOUR TRANSMISSION RATE:

There are two standard test procedures for figuring out water vapour transmission rate. The two techniques are ISO 11092 and ASTM E96. Both approaches take a lot of time, and aren't suitable due to a lot of test parameters. We were able to quickly measure the water vapour permeability of prepared lyophilized wafers subjected to constant temperature and humidity due to a substantially faster test procedure using a modification of the standard test methods. [76]

The cup filled with distilled water had the film sealed on it. After that, the temperature was adjusted to room temperature and the cup was put in the desiccator to keep the humidity constant. The desiccator's relative humidity was stabilized with the use of silica beads at the base of the desiccator. Periodically, the cups were taken out and weighed. The amount of

water lost from the cups in relation to time was then determined. [77] The formula below was used to get the water vapour transmission rate:

$$\mathbf{WVTR}=\frac{(W/t)}{A}$$

Where,

WVTR: water vapour transmission rate (g/m^2·d)

W: change in weight (g)

t: time (in days)

$\frac{W}{t}$: weight loss per day (g/d)

A: test wafer area (m^2)

5.3.8. TG-DTA:

The thermal behaviour was investigated using an aluminium crucible on a Perkin Elmer TG/DTA Diamond Thermal Analyser. The wafer samples were analysed in a dynamic air environment (synthetic air 5.0 Linde Gas with flow 100 mL·min−1). [78] Samples were prepared for TGA analysis by equilibrating them at 30 ◦C and heating them to 300 °C at a rate of 10 °C/min, while monitoring the weight loss. Nitrogen flow was set at a rate of 30 mL/min. [79] Exothermic and endothermic events were identified using calculated differential thermal analysis (c-DTA). DTA was used in these observations to perform multiple-point temperature calibration. The starting temperatures of the melting peaks of high-purity reference materials (In, Sn, Zn, Al, BaCO3, and Au) were found for this approach across the whole temperature range. Similar thermal parameters were considered for all tested samples. [80]

5.3.9. X-RAY DIFFRACTION (XRD):

The physical form (amorphous or crystalline) of the pure drug, Blank, and 100mg drug-loaded wafers was examined using XRD. Using a glass slide, the wafers were compressed to cover the holder's round tiles. Transparent plastic cling film was then used to safely attach the wafers to the sample cells. The D8 Advance X-ray diffractometer was used in transmission mode for the experiment. The instrument had a primary solar slit of 4° and a secondary solar

slit of 2.5°, with an exit slit of 0.6 mm. The voltage and current settings were 40 kV and 40 mA, respectively. [81]

5.3.10. FOURIER TRANSFORM INFRARED SPECTROSCOPY (FTIR):

The wafers were characterized using an FTIR spectrophotometer and a ZnSe attenuated total reflectance (ATR) accessory. Potassium bromide (KBr) beam splitter and MCT detector were installed on the FTIR. Wafers (Blank, F1, F2, F3) were positioned on a 45-degree ZnSe ATR crystal, and maximum pressure was applied using a pressure clamp accessory to provide close contact between the wafers and the crystal. In a similar manner, curcumin (drug) alone was examined as a control. OMNICR software was utilized to record spectra at a resolution of 4 cm^{-1} over a range of 650–4000 cm^{-1}. Each sample's true absorbance was calculated by removing the ATR crystal's background spectrum information. [82]

5.3.11. SCANNING ELECTRON MICROSCOPY (SEM)

For the SEM analysis, blank, F1, F2 and F3 formulations were taken. Double-sided adhesive carbon tape was applied to labelled stainless steel stubs to prepare the exterior surfaces of the lyophilized wafers for SEM analysis. With caution not to harm the wafers' surface topography, the samples were positioned on the exposed side of the carbon adhesive. Next, these were put inside the Field Emission Scanning Electron Microscopy (FESEM) (Class One Equipment) chamber after sputter coating with thin layer of electrically conductive gold under a vacuum for charge neutralisation.[83]

5.3.12. ANTI-MICROBIAL STUDY:

The disc diffusion method was used to test the effectiveness of the antimicrobial property of the drug. Gram-positive B. subtilis and Gram-negative Escherichia coli were the two types of bacteria that were selected. Müller Hinton (MH) agar was utilized for the tests of antimicrobial effectiveness and inoculation, whereas nutrient agar was employed as the culture medium. The antimicrobial wafer was punched into discs with a 6 mm diameter.

The turbidity of the suspension suggested that there were $1x10^8$–$2x10^8$ CFU/mL of B. subtilis or E. coli in the bacterial suspension. The bacteria multiply quickly, thus the suspension was used within 15 minutes after preparation.

Using the disc diffusion method for antimicrobials, the dried surface of the MH agar plate was infected by streaking the sterile swab over the entire surface three times after dipping it into the inoculum tube. Approximately sixty rotations of the plate were performed to guarantee uniform dispersion of the inoculum. Before the disc was placed, the agar surface was left to dry for three to five minutes at room temperature. To guarantee full contact between the wafer disc and the agar surface, the antimicrobial-containing wafer disc was placed onto the dried agar surface and carefully pushed with forceps.

Three identical wafer samples (selected randomly from Blank, F1, F2, and F3) were present in each petri dish. Following which, the plate was turned over and incubated for twenty-four hours at 35 ± 2°C. After incubation, the diameter of the disc was used as a reference to measure the zone sizes with a ruler. The zone of inhibition diameter for both the bacteria was determined. [84]

IN-VITRO DRUG RELEASE STUDY:

USP Paddle-over-disc Type Dissolution Apparatus was used for the in vitro study. The set up was simulated by placing the lyophilized wafers (F1, F2 and F3) in a Petri dish and a muslin cloth was tied around it to act as a semi permeable membrane. Lyophilized drug wafers were thus exposed to phosphate buffer (pH 7.4) across the muslin cloth. Every dissolution study was conducted at 37 ± 0.5 °C at 50 rpm, with 900 ml of phosphate buffer inside every dissolution jar. Samples of 1 ml each were taken out at regular time intervals and diluted with 9ml buffer solution and subjected to analysis at 429 nm using a UV spectrophotometer against a standard buffer solution. The sink condition was maintained throughout the dissolution process.

RELEASE KINETICS:

A kinetic model can help explain the pharmacokinetics of a drug delivery carrier. The volume, solubility, crystallinity, and size of the drug, together with the kind of carrier the drug is encapsulated in, all significantly influence how the drug releases from the formulation. The kinetics of drug release are described by a variety of kinetic models, including zero-order ($Qt = K0t + Q0$), first-order ($Qt = Q0e^{-Kft}$), Higuchi ($Qt = KH^{-t} + Q0$), Korsmeyer-Peppas ($Qt/Q\infty = Kktn$), and Hixon-Crowell ($Q01/3/Q\ t1/3 = Kst$). The amounts of drug released at time t (Qt), the initial amount (Q0), and the release rate constants (K0, Kf, KH, Ks, Kk) for zero-order kinetics, first-order kinetics, the Higuchi model, the Hixon-Crowell model, and the Korsmeyer-Peppas model are all included in these equations.

CHAPTER 6:

RESULT AND DISCUSSIONS

6.1. PRE-FORMULATION STUDY

6.1.1. PHYSICAL CHARACTERIZATION:

The physical characterization of the drug, curcumin for colour, texture and odour was studied, which showed all acceptable results that complies as per IP standards.

Sl. No.	Property	Observation
1	Texture	Hard and Dense Powdery.
2	Colour	Bright yellow colour.
3	Odour	Earthy Mustard-like

Table 3: physical characterization of drug.

6.1.2. MELTING POINT OF DRUG:

Melting points are frequently used to determine the purity and characteristics of both organic and inorganic crystalline substances. When it comes to melting, pure substances have a very narrow melting range (0.5–1 °C), while contaminated and impure compounds typically show a wider melting range. Generally speaking, a contaminated substance melts at a temperature that is lower than a pure substance. Melting point depression is the term for this characteristic, which can be utilized to gather qualitative data regarding a substance's purity. [85]

The melting point of the drug, curcumin was found to be 168ºC which was slightly below the ideal curcumin melting point 179ºC - 182ºC. [86] This may be due to minute degradation of the drug. But being within acceptable range, the drug, curcumin is used for encapsulation within the lyophilized wafer.

Standard curve of curcumin in mixture of Phosphate buffer 7.4 and ethanol:

Determination of a standard calibration curve was performed using a 1:1 mixture of phosphate buffer (7.4) and ethanol to determine the drug's release profile and efficiency of entrapment. The curcumin standard solution's UV-visible absorbance demonstrated linearity at λ_{max} 429 nm within the range of 2–20 µg/ml of medication. The linear equation (y = 0.0324x - 0.0458) was discovered and R^2= 0.9989.

Concentration	Absorbance
2	0.029
4	0.083
6	0.145
8	0.212
10	0.274
12	0.342
14	0.400
16	0.479
18	0.532
20	0.613

*Table 4***:** Absorbance of aliquoits of curcumin at λ_{max} 429nm.

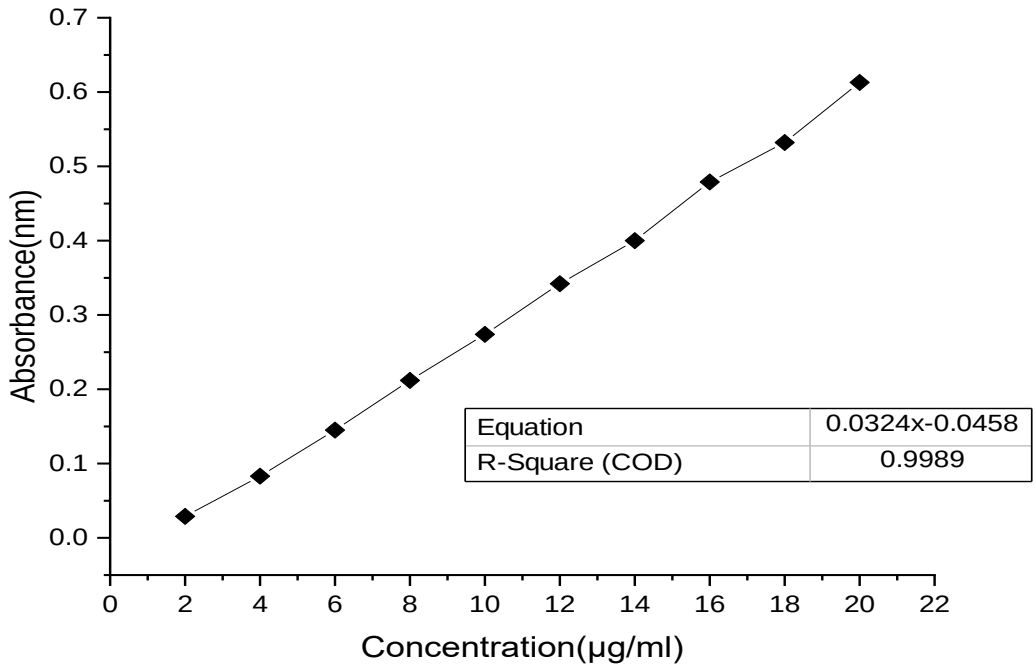

Figure 4: Standard Calibration curve of curcumin in 1:1 mixture of phosphate buffer (7.4) and ethanol.

6.2. CHARACTERIZATION:

6.2.1. THICKNESS:

Since the accuracy of the dose in the wafer is closely correlated with the uniformity of the wafer's thickness, this is crucial to determine its thickness. [87] Average thickness of different wafers were determined and the blank wafer showed highest thickness; which might be due to lesser overall concentration of the formulation mixture. Moreover each of the wafers showed significantly similar thickness all around the wafer surfaces.

Sample	**Location 1**	**Location 2**	**Location 3**	**Location 4**	**Average thickness(mm)**
Blank wafer	1.10	2.63	2.30	1.59	1.905
F1	1.98	1.82	0.81	0.69	1.335
F2	1.16	1.58	1.10	1.48	1.385
F3	0.78	0.87	1.36	1.22	1.057

Table 5: shows thickness of Blank, F1, F2 and F3 formulation taken at four different location of the wafer.

6.2.2. DENSITY:

The density of the lyophilized wafer is used to signify how uniformly the drug is incorporated all throughout the wafer surface. The density of all the samples are given in the following table:

Sample	**Density(g/cm^3)**
Blank Wafer	0.136
50mg Wafer	0.201
100mg Wafer	0.183
150mg Wafer	0.256

Table 6: shows density of Blank, F1, F2 and F3 formulation.

6.2.3. FOLDING ENDURANCE:

A film's capacity to tolerate repeated bending and folding is determined by its folding endurance. The soft and flexible film was indicated by the higher folding endurance score.

This characteristic varies according to the kind of plasticizer and polymer utilized. Formulation F1 was found to have better folding endurance which indicates better patient compliance; and it requires lesser necessity for reapplication. [73]

FORMULATION	FOLDING ENDURANCE
BLANK	50
F1	42
F2	23
F3	20

Table 7: shows folding endurance of Blank, F1,F2 and F3 formulation

6.2.4. PERCENTAGE YIELD:

The percentage yield of the lyophilized wafer is demonstrated in table 8. Percentage yield calculates a chemical reaction's efficiency. It provides us with the percentage of our reactants that were successfully converted into a product. The table depicts that F3 formulation has the highest percentage yield and least loss of ingredients.

Sample	Percentage yield (%)
F1	89.94
F2	93.685
F3	94.085

Table 8: shows the percentage yield (%) of Blank, F1, F2 and F3 formulation.

6.2.5. SWELLING INDEX (%) DETERMINATION:

The swelling is a crucial feature for hydrophilic polymer-based matrices, like the Lyophilized wafers developed in the present study, since it influences other functional attributes like mucoadhesion, disintegration rate, drug dissolution, and ultimately release from the swollen wafer. It is dependent upon a number of physical characteristics, such as mechanical strength, porosity, and matrix density, etc. Increased chain mobility, resulted from moisture absorption during swelling causes polymer chains to change from a glassy to a rubbery state. [88]

The figure 5 shows swelling index of blank wafer, F1, F2 and F3 formulation. It depicts that higher curcumin (drug) content shows lower swelling index which may be due to the lower

solubility and stability of curcumin in aqueous media. [89] Moreover with increase in time, the swelling profile shows higher values. Thus F1 formulation shows the highest swelling index and thus better swelling properties as compared to F2 and further more from F3. These data signifies that curcumin wafer formulated with hydrophilic polymeric mixture is suitable for potential release of curcumin. [88]

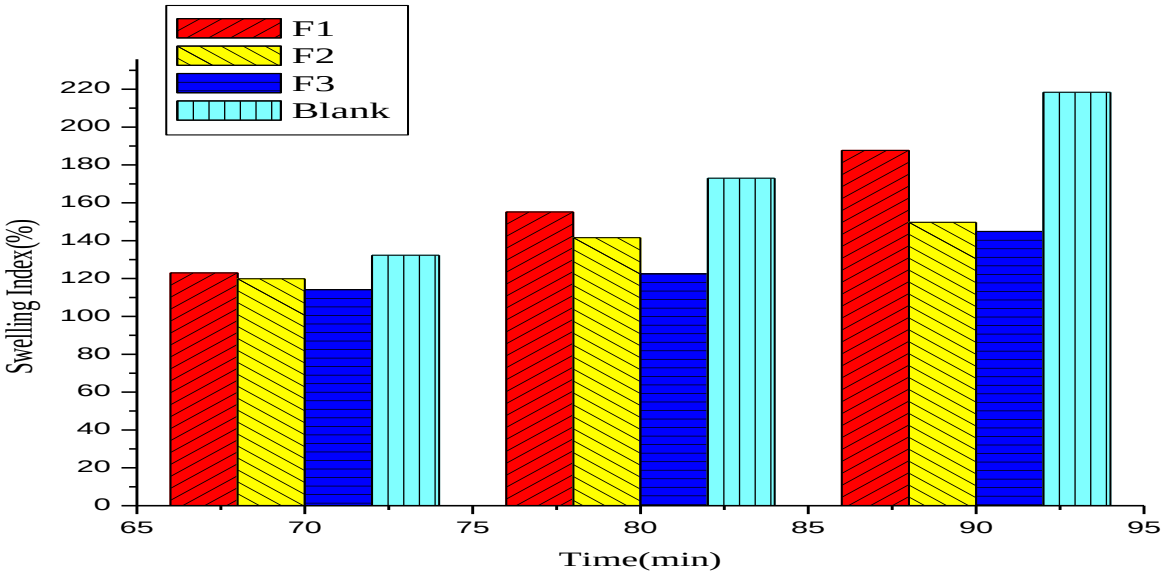

Figure 5: shows Swelling index of Blank, F1, F2 and F3 wafer formulation.

6.2.6. TENSILE STRENGTH:

Figure 6 shows the texture analysis of the lyophilized wafer (F1, F2, F3) by comparing their tensile strength and extensibility. It is demonstrated that with increase in drug (curcumin) content in the wafer, the tensile strength is shown to decrease with increase in its extensibility. This phenomenon can be due to the hydrophobicity of curcumin. Thus F1 formulation having lower hydrophobic drug content have higher tensile strength than F2 or F3. The extensibility of the wafer formulation was shown to be negligible due to the porous and rigid nature of the wafer. [90]

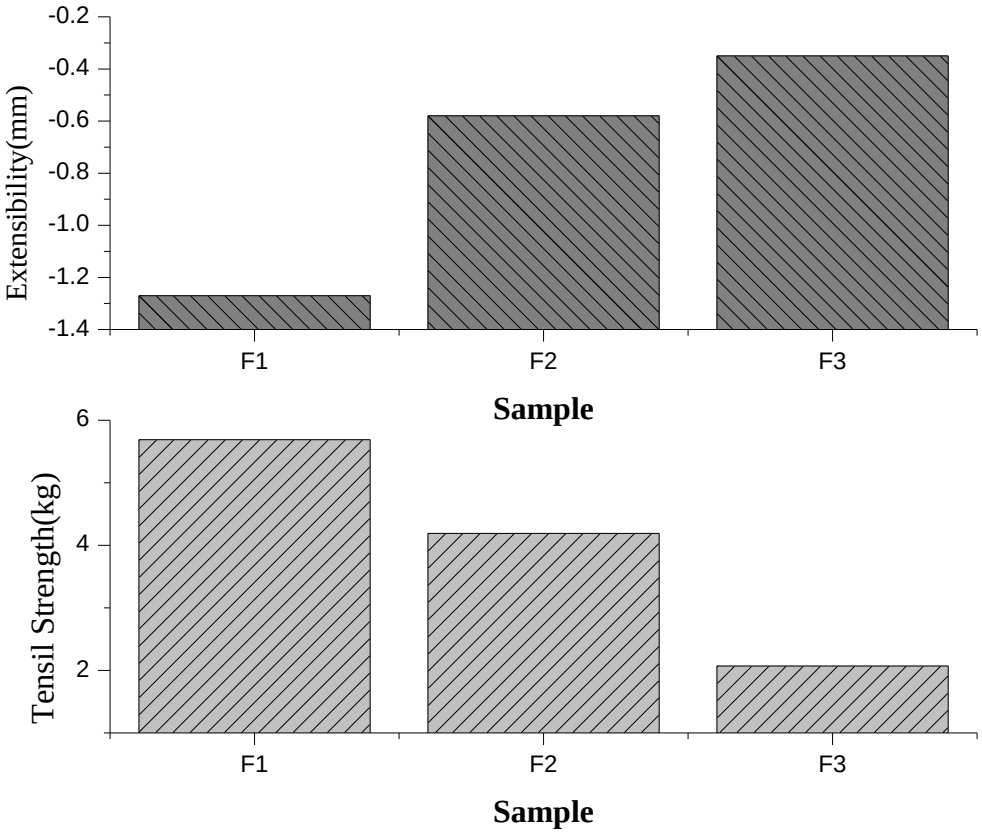

Figure 6: shows tensile strength and extensibility comparison between the three drug loaded wafers

6.2.7. WATER VAPOUR TRANSMISSION RATE:

The constant flow of water vapour through a unit area of the object in a unit of time, through a certain parallel surface, under particular temperature and humidity conditions is known as the water vapour transmission rate.

In order to prevent exudate accumulation at the wound site, a wound dressing should be able deliver the ideal water vapour transmission rate. After eight days of loss of water vapour, the WVTR of Blank, F1, F2, and F3 were respectively found to be, 628.932, 574.305, 543.059, and 530.213 (g/m^2/day). Study results showed that every lyophilized wafer had the ability to permeate water vapour through them, optimally. Sustaining proper moisture levels is crucial for the healing process because it promotes migration of cell and aids in the epithelialization of the wound site.

Research indicates that the WVT rate for uninjured skin is 204 g/m^2/day, but for first-degree burns and granulating wounds, it varies from 279 to 5138 g/m^2/day. The wafer formulations

employed in the current study had WVT rates between 530.213 and 628.932 g/m2/day. It showed that the wafer formulations could keep low to medium level exudative wounds moistened at the wound site without severely dehydration, by being sufficiently permeable to water vapour. Furthermore, the outcomes demonstrated that the WVTR of the different wafer compositions had significantly similar results. [91]

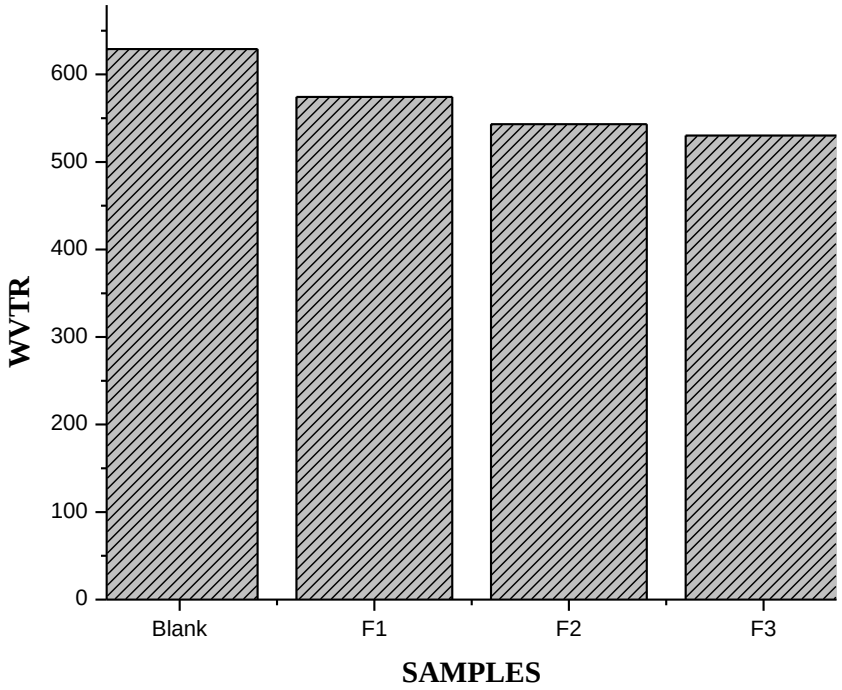

Figure 7 shows comparison of WVTR of Blank, F1, F2 and F3 formulation after 8 days of reading.

6.2.8. TG-DTA:

Figure 8 shows the TG/DTA curve of Blank wafer, pure drug and F2 formulation wafer. On comparing the TGA data between blank wafer and drug loaded lyophilized wafer from the figure 8.A, it can be depicted that the thermal degradation process of blank wafer can be divided into two stages; first stage being between 58ºC - 85ºC which shows free water and bound water volatization and the second stage degradation was between 235ºC - 315ºC which may be due to the degradation and depolymerisation process of lyophilized wafer formulation.

Whereas, in drug loaded wafer it showed first degradation stages due to the evaporation of volatile compound occurred around 40ºC-110ºC. Between 200ºC to 320ºC the second degradation stage signifies the degradation of the lyophilized wafer. The drug free and drug loaded wafer showed identical Thermal Decomposition ($T_{0.5}$) which shows no change in thermal stability of lyophilized wafer when curcumin is added to it. [92]

The DTA Curve of pure curcumin showed sharp endothermic peak at 174ºC associated with the melting point of curcumin whereas a wide exothermic peak at 260ºC shows the thermal degradation of the drug. [80] Moreover, the DTA curve of both drug free and drug loaded wafers showed similar exothermic peaks near 250ºC, which also confirms curcumin's inability to hamper thermal integrity of the lyophilized wafer.

A.

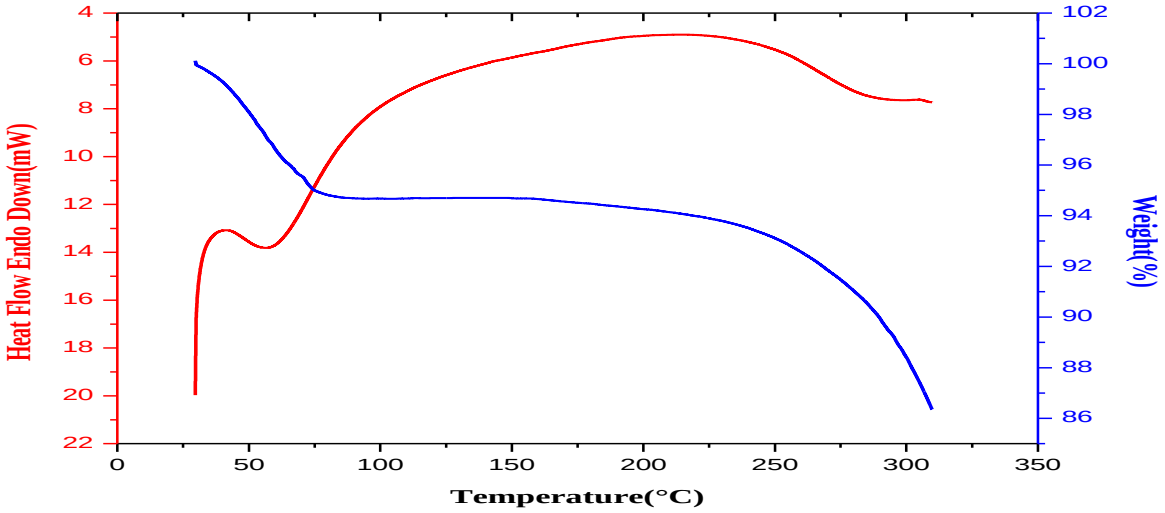

B.

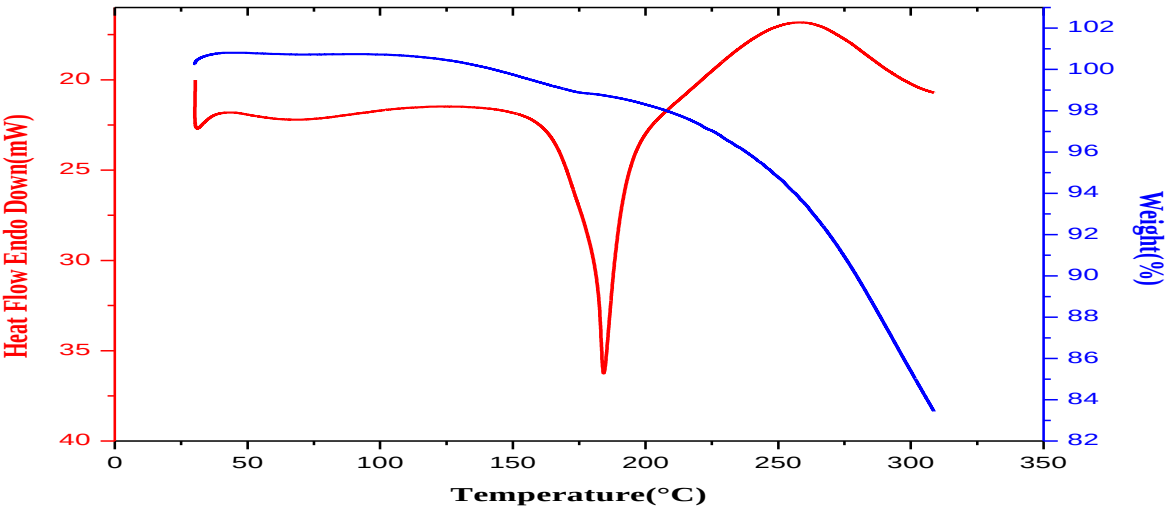

C.

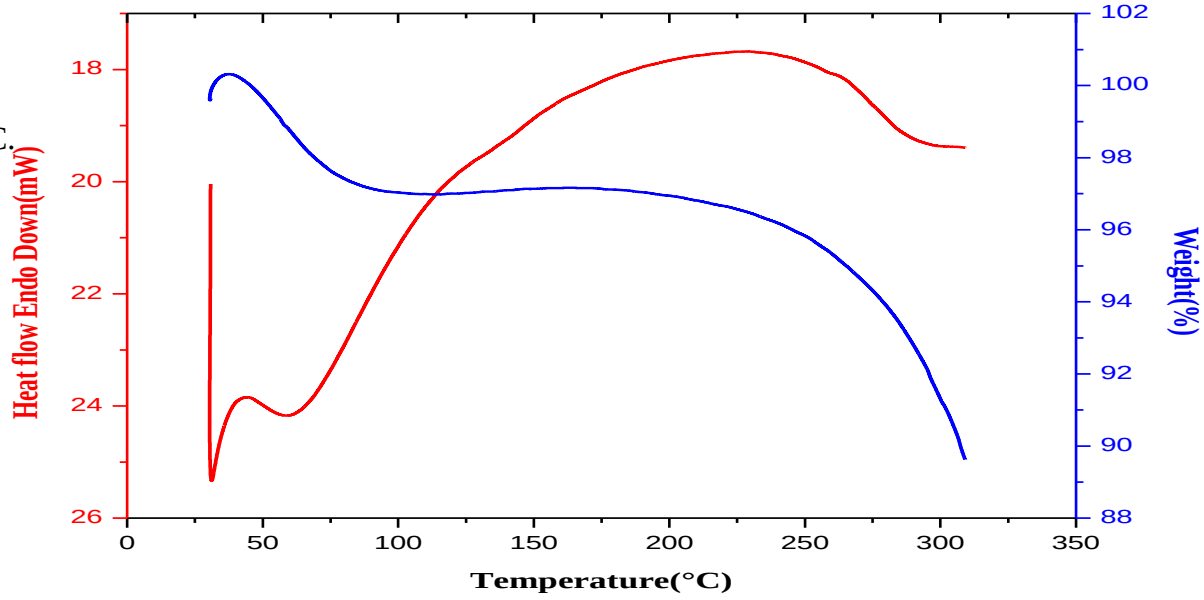

Figure 8. Shows TG/DTA graph of (A) blank wafer (B) pure drug and (C) F2 formulation.

6.2.9. XRD:

Figure 1(A)(B)(C) shows XRD defration pattern for pure drug, Blank wafer and F2 wafer. The drug (curcumin)'s XRD patterns are displayed in Figure 1(a). For these samples, XRD analyses were performed in order to comprehend the crystallinity changes. The crystalline nature, significant strains, anisotrophy and texture of the sample can be understood by evaluating the defraction-peak, width, intensity, and position on the scale. Sharp, intense peaks at 2ɵ values, 8.851, 12.193, 14.440, 17.177, 18.197, 21.161, 23.332, 23.748, 24.503, 25.523, 26.146, 27.354 and 28.883 on the graph suggested that the medication was in its crystalline form.

The diffractogram in figure 9B shows the XRD curve of the blank wafer; the curve signifies lack of sharp peaks showing the amorphous nature of the polymeric mixture. Two broad peaks at around 2ɵ value 10 and 22 might be due to formation of a leafy arrangement on top of one another caused by compression, thus resulting in detection of false crystalline peak. Similar curve is obtained in drug loaded lyophilized wafer confirming its amorphous structure. Disappearance of sharp peaks that appeared in case of curcumin, is mainly due molecular dispersion of drug inside the polymeric mixture of the lyophilized wafer. [93] This can be justified due to the homogenization step of the drug loaded polymeric mixture before freeze drying.

A.

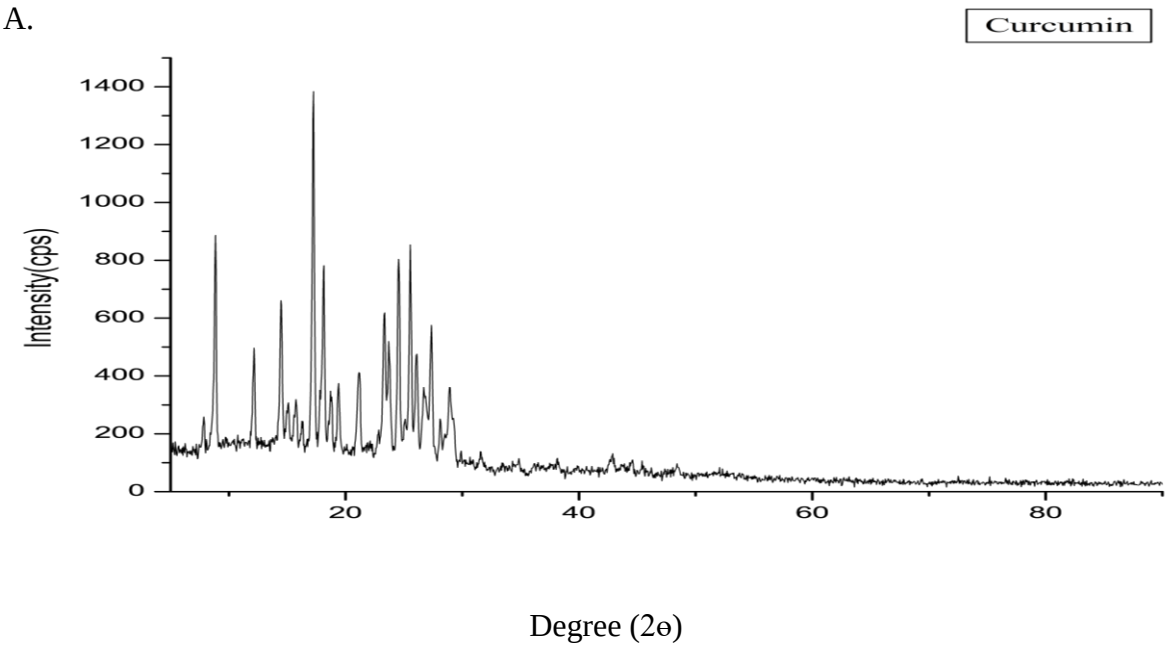

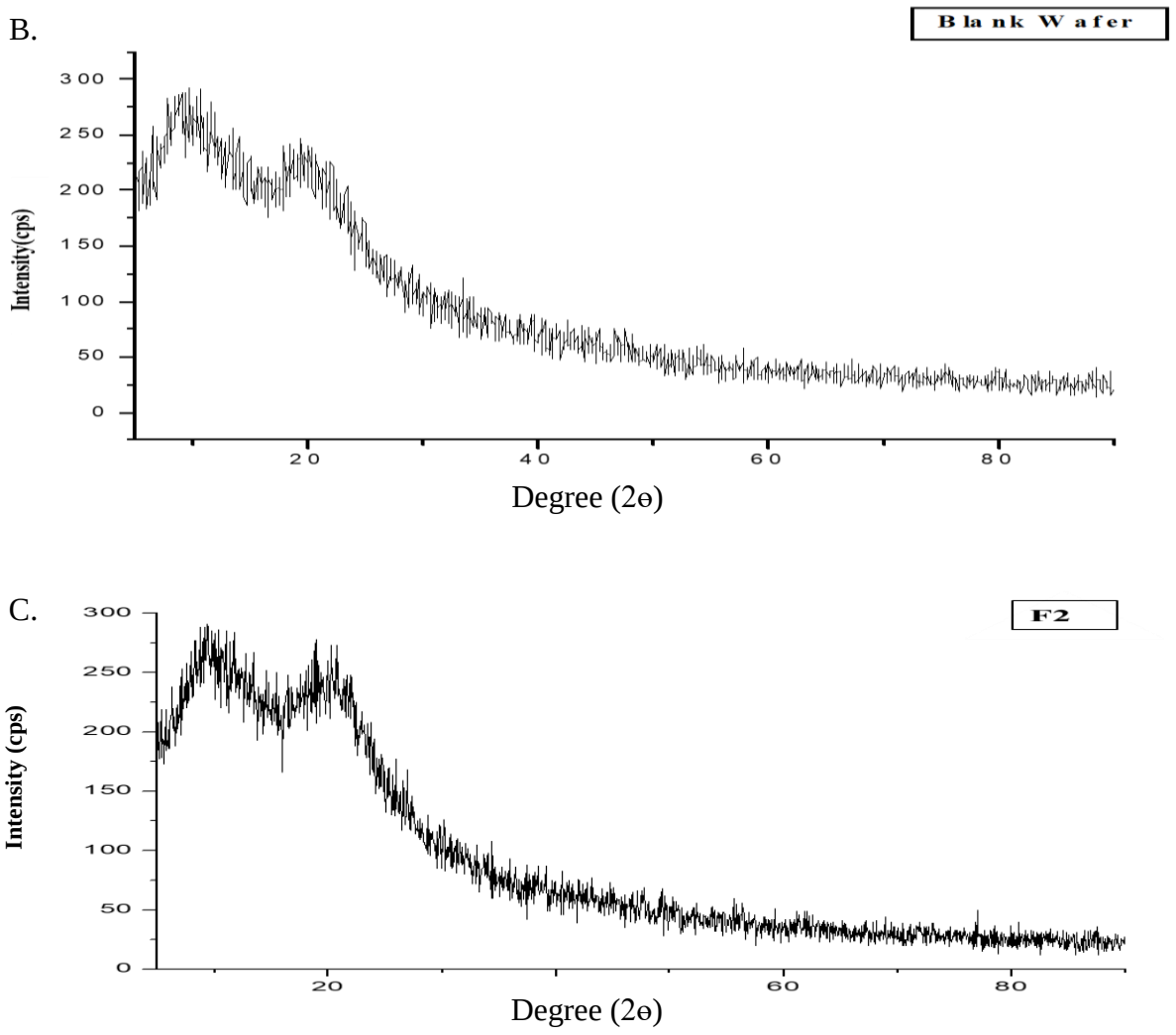

Figure 9- shows XRD graph of (A) curcumin; (B) blank wafer; (C) F2 formulation

6.2.10. FTIR:

Figure 10 displays the FTIR spectra of the drug in its pure form, and different polymers such ethyl cellulose, HPMC and PVP in different lyophilized wafers with varying amounts of drug (blank, 50mg, and 100mg) and their interactions.

In figure 10(A), the major peaks of pure curcumin were observed at approximately 3510.45 cm^{-1}, which was attributed to the phenolic O-H stretching vibration; sharp absorption bands at 1602.85 cm^{-1}, which was attributed to the benzene ring's stretching vibrations; 1510.26 cm^{-1}, which was attributed to the C = O and C = C vibration; 1429.25 cm^{-1}, which was attributed to the olefinic C–H bending vibration; 1282.66 cm^{-1}, which was attributed to the aromatic C–O

stretching vibration; and 1028.06/856.39 cm^{-1}, which was observed due to the C–O–C stretching vibrations of the curcumin. [94]

Figure 10(B) FTIR spectra for ethyl cellulose depicted the OH groups that are responsible for the prominent peak that was seen at 3475.73 cm^{-1}. While CH_3 bending is responsible for the peak at 1382.96 cm^{-1}, CH stretching may be the cause of the asymmetric peak in the 2970–2870 cm-1 area. The little peak at 1467.83 cm^{-1} is caused by the bending of CH_2. [95] The natural HPMC sample displayed peaks at 3475.73 cm^{-1} as a result of intermolecular H-bonding and OH stretching vibration. The stretching vibration of the -CH is responsible for the peak at 2941.44 cm^{-1}, while the existence of C=O stretching of the carbonyl group is indicated by the band at 1639.49 cm^{-1}. [96] For the distinctive peaks of PVP, 3431.36 cm^{-1} (-OH stretching vibration), 1639.49 cm^{-1} (C=O stretching vibration), and 1294.24 cm^{-1} (C-N stretching), are seen. The symmetric and asymmetric stretching vibrations of CH_2 are associated with the peaks located at 2958.80 and 2887.44 cm^{-1}, respectively. [97]

The curcumin loaded wafers demonstrated in fig. 10(C) and 10(D) a broad peak that signifies interaction of curcumin with the polymeric mixture of EC, HPMC and PVP around 2700cm^{-1} to 3700cm^{-1}. The other interaction is depicted by shifting of peaks attributed to benzene ring's stretching vibration of curcumin to higher wave number at around 1600 cm^{-1} from 1510.26cm^{-1}. In both the figures C and D, the peaks between wavenumbers 2700cm^{-1} and 3000cm^{-1} represents asymmetric and symmetric stretching vibrations of CH group and CH_2 group that has shown very slight shifts but higher intensity with higher amount of curcumin incorporation. The peak for stretching vibration of C-O-C of curcumin at 1028.06/856.39 cm^{-1} showed increase in intensity of peaks with higher drug content in wafers. Few missing peaks of curcumin depicted incorporation of the drug into the lyophilized wafer thus showing good drug loading capacity of the wafer.

Following are the ATR–FTIR spectra showing peaks for different components within freeze-dried wafers:

A.

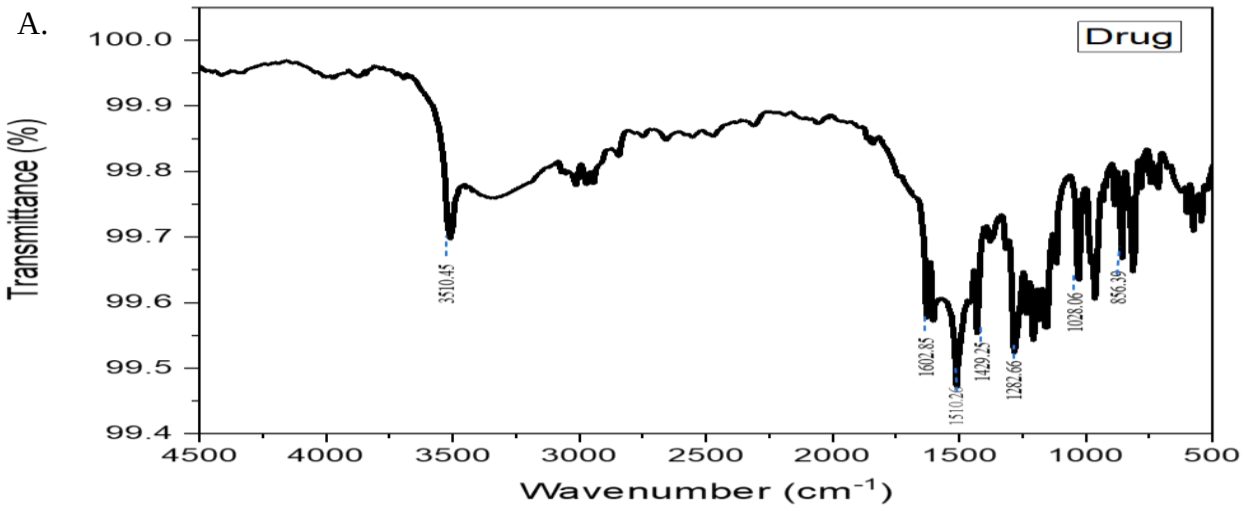

B.

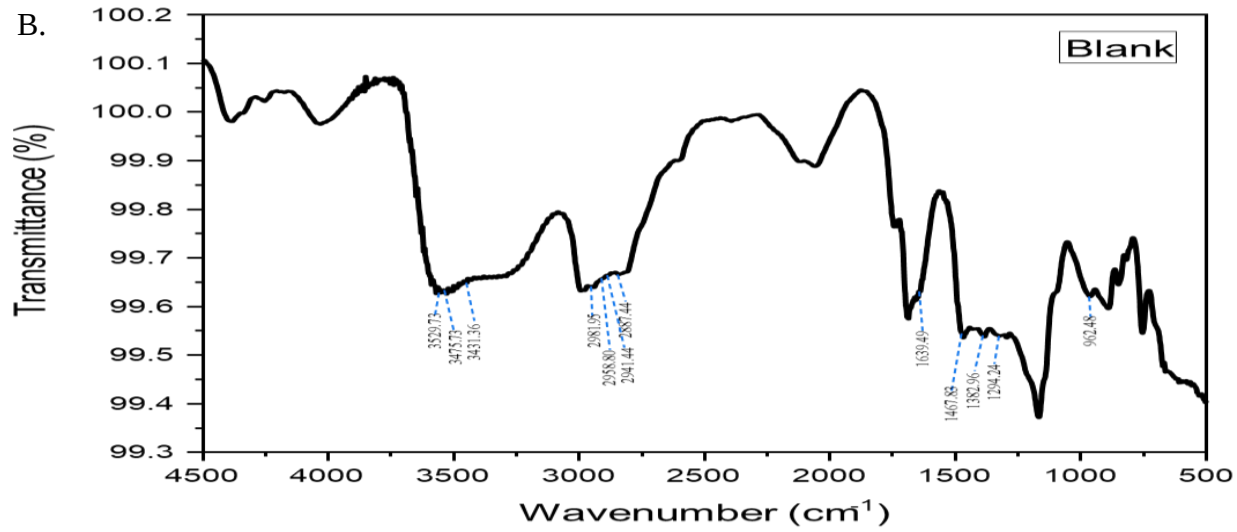

C.

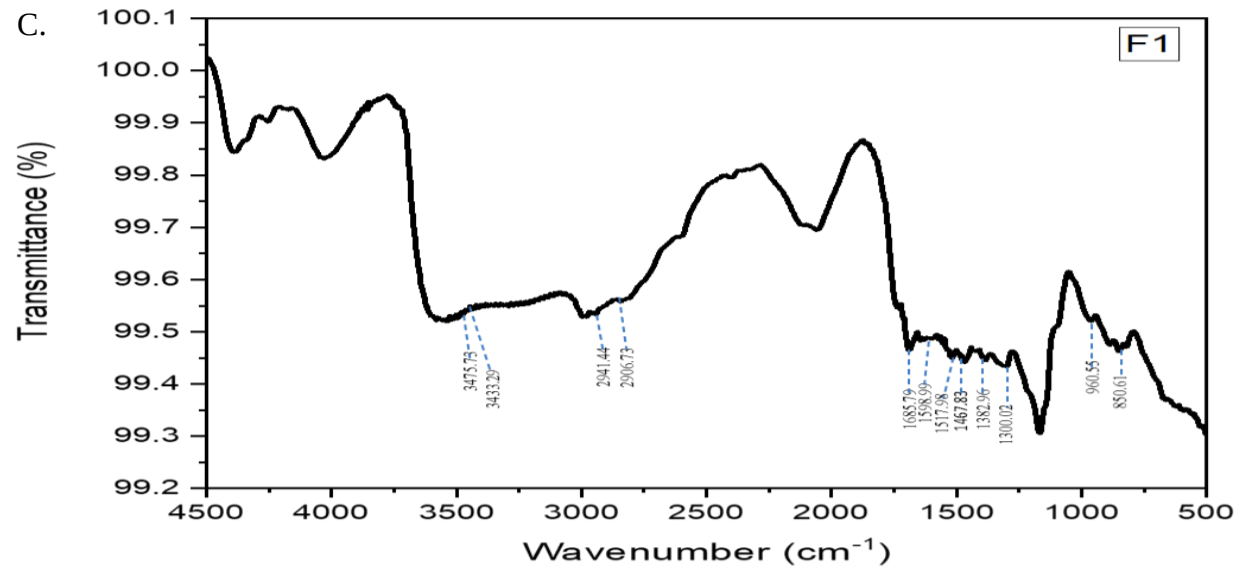

D.

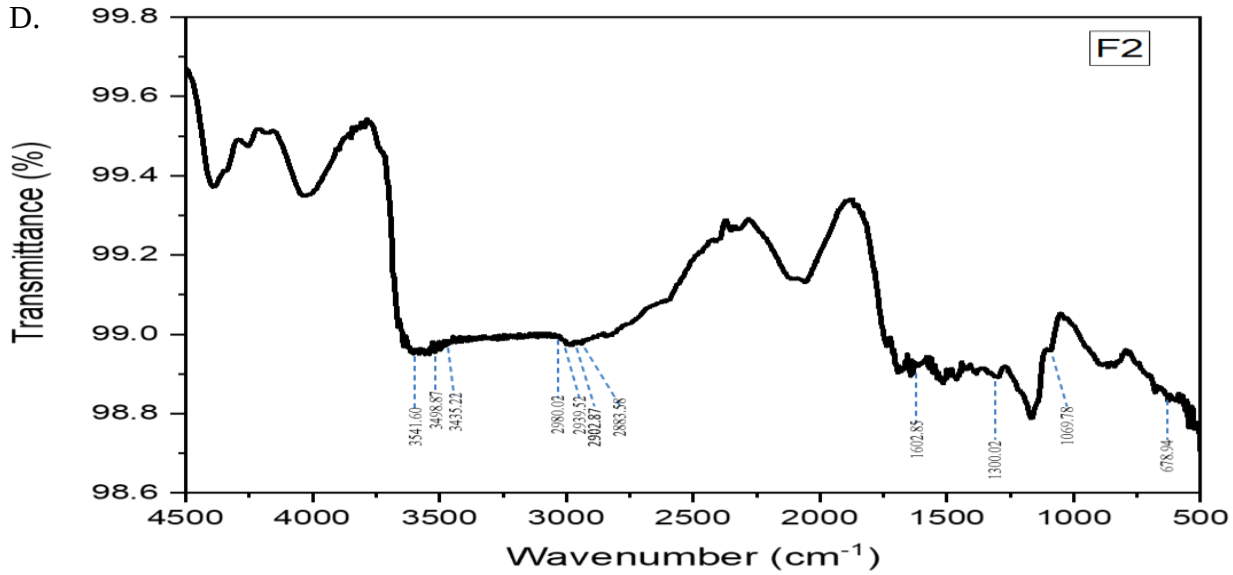

Figure 10 shows the ATR–FTIR spectra showing peaks for different components within (A) Drug, (B) Blank, (C) F1 and (D) F2.

6.2.11. SCANNING ELECTRON MICROSCOPY (SEM):

Figure 11 illustrates how different polymer compositions and drug dosages affect the pore diameters of lyophilized wafers, as determined by SEM study. The blank and F1 formulation wafer's morphology shows an interconnected network with some irregular shaped, microscopic pores.

A denser network with a mixed sized pores were seen upon increasing the drug dosage by 50 mg of curcumin on each consecutive wafers. Thus, F3 formulation, followed by F2, showed highly dense, porous structure with highest number of spherical drug particles entrapped amidst them. The complex porous structure, most evidently visible in the F2 and F3, but also present in blank and F1, is due to sublimation of bound and unbound solvent from the polymeric mixture by the lyophilization process. [98]

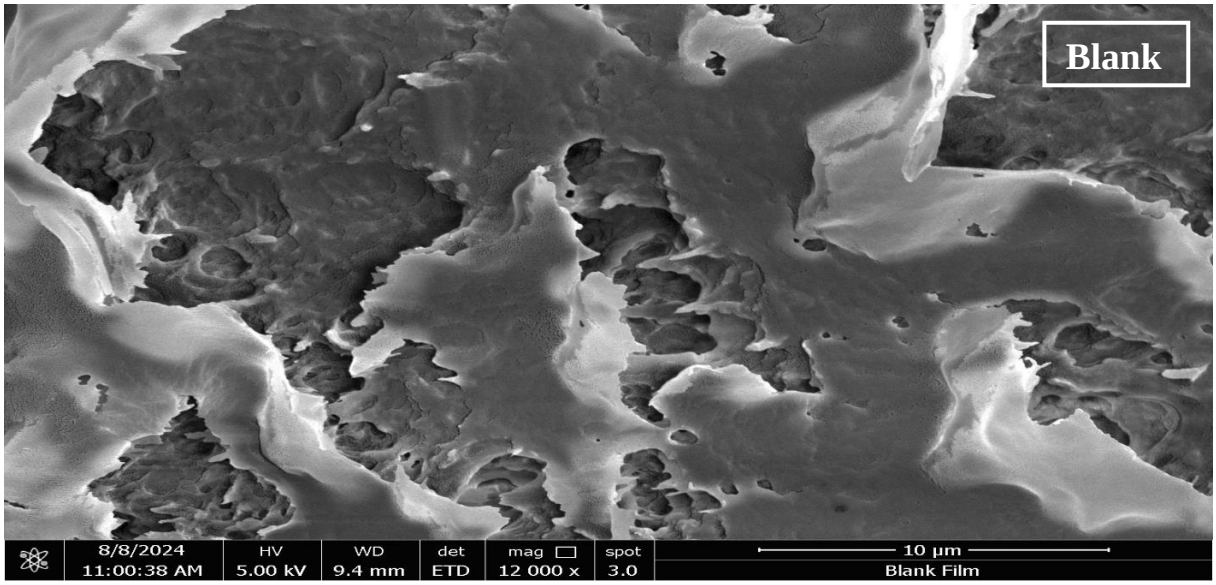
Blank
8/8/2024
11:00:38 AM
HV
5.00 kV
WD
9.4 mm
det
ETD
mag
12 000 x
spot
3.0
10 µm
Blank Film

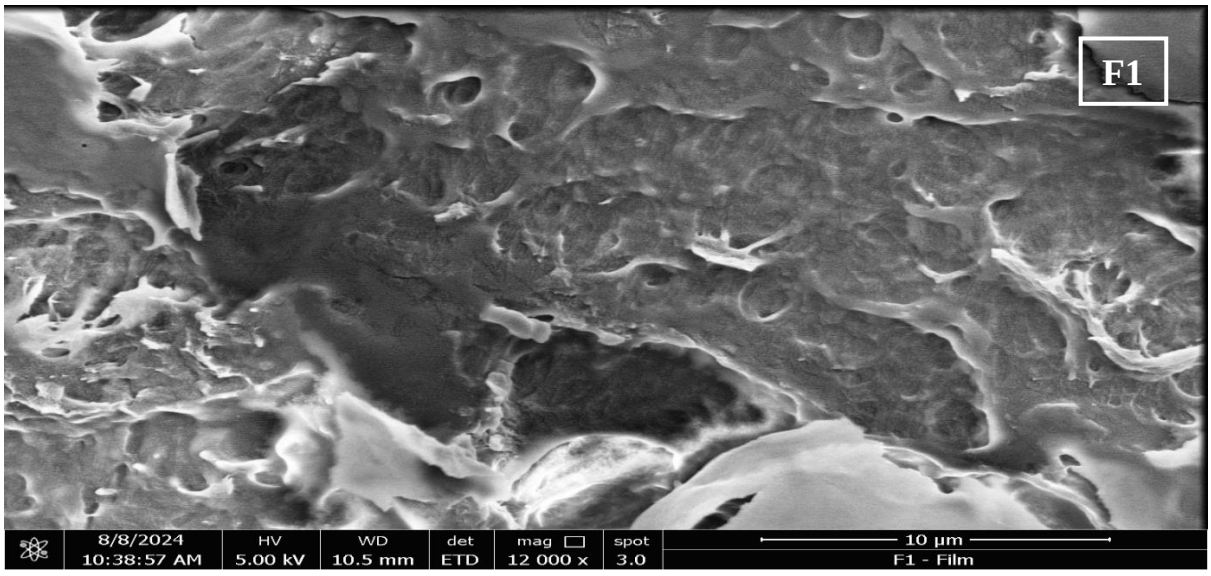
F1
8/8/2024
10:38:57 AM
HV
5.00 kV
WD
10.5 mm
det
ETD
mag
12 000 x
spot
3.0
10 µm
F1 - Film

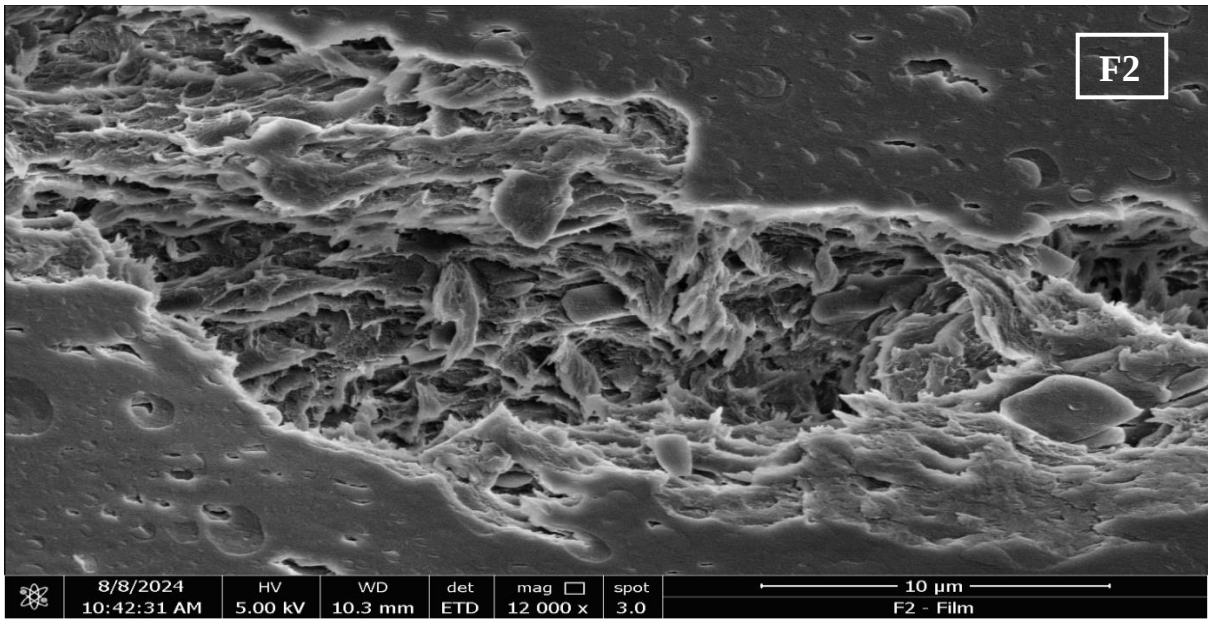
F2
8/8/2024
10:42:31 AM
HV
5.00 kV
WD
10.3 mm
det
ETD
mag
12 000 x
spot
3.0
10 µm
F2 - Film

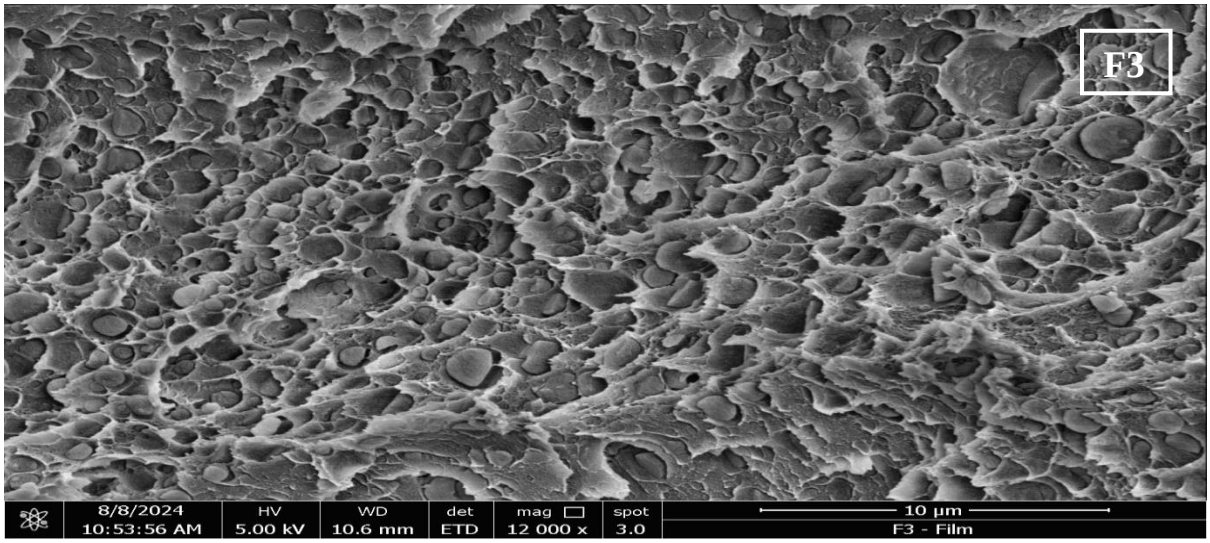

Figure 11 depicts SEM images of Blank, F1, F2 and F3 formulation.

6.2.12. ANTI-MICROBIAL STUDY:

The figure 12 depicts diameter for zone of inhibition of bacterial growth, for E. Coli and B. Subtilis, by curcumin loaded lyophilized wafer on the MH agar surface. For the inhibition of gram positive bacteria, *B. Subtilis*, F3 formulation showed largest zone (9.5mm) and F1 showed smallest zone (6mm). Similarly, for the inhibition gram negative bacteria, *E. Coli*, F3 formulation showed largest zone (9mm) and F1 showed smallest zone of inhibition (5.7mm). This may signify that with increase in curcumin content in wafers, the zone of inhibition of bacteria increased, thus showing the antimicrobial property of curcumin in the prepared wafer. Moreover the blank wafer showed no zone of inhibition due to absence of curcumin in it. Thus F3 formulation showed best antimicrobial property. [84]

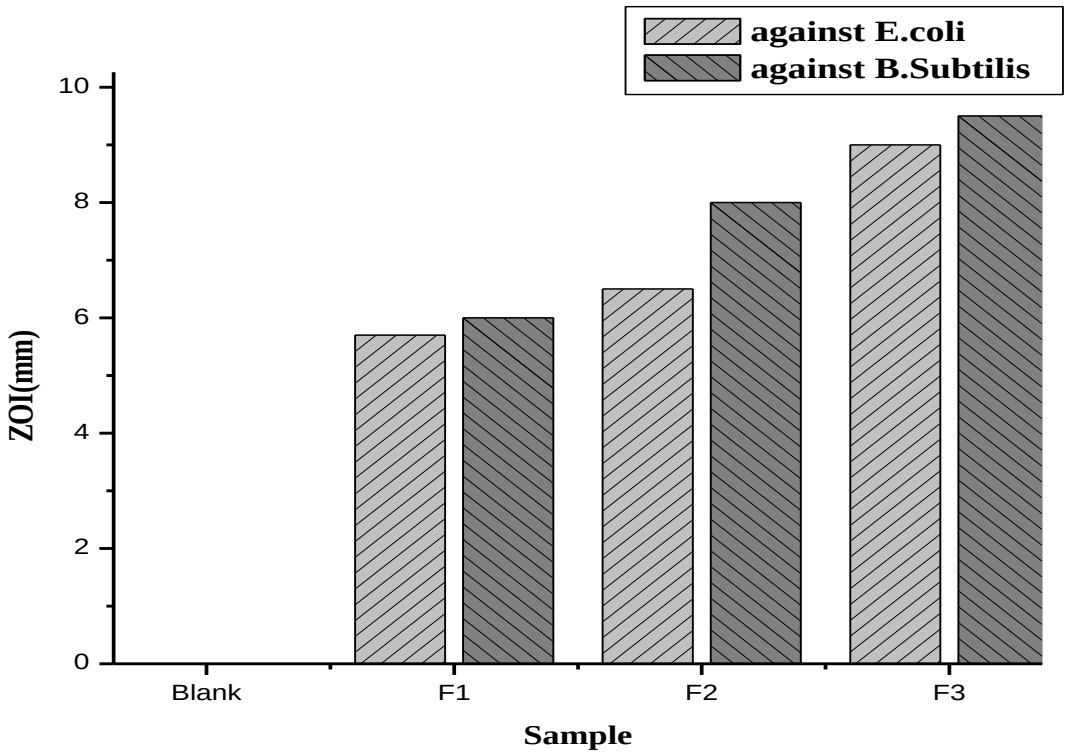

Figure 12: shows zone of inhibition of Blank, F1, F2 and F3 formulation for anti-microbial study.

IN VITRO DRUG RELEASE STUDY:

The in vitro release study of formulated lyophilized wafers namely F1, F2, and F3, was conducted to assess their drug release profiles. After an initial 4-hour observation period, it was observed that F1 exhibited a drug release of 32.58%, F2 released 27.72% of the drug and F3 released 20.5%. Subsequently, the study extended for another 4 hours, totalling 8 hours of examination. At the end of this extended period, the drug release percentages were as follows: F1, 39.53%; F2, 35.36% and F3, 23.86%.

It can be found that increased concentration of drug in F2 and F3 formulations has not enhanced drug release but rather has decreased drug release from wafer formulations. It may be due to more curcumin (a hydrophobic drug) in the pores of the wafer, which has prevented the entering of water or media into it. As a result, carrying of drug from the three-dimensional scaffold (wafer) by diffusion process is hindered.

Notably, over the course of 8 hours, the curcumin dissolved gradually in the release media—there were no sudden burst effect. The curcumin loaded porous matrix thus prepared within the wafers can be used as a potential antibacterial wound dressing with slow drug release and quick relief from bacteria and inflammation due to these release patterns.[99]

Time (hr)	Absorbance	Concentration (µg)	Cumulative amount in 900ml	Cumulative concentration in mg	Cumulative % drug release
1	0.027	2.24691358	2022.222222	2.022222222	20.22222222
2	0.051	2.987654321	2688.888889	2.688888889	26.88888889
3	0.0635	3.37345679	3036.111111	3.036111111	30.36111111
4	0.0715	3.62037037	3258.333333	3.258333333	32.58333333
5	0.081	3.913580247	3522.222222	3.522222222	35.22222222
6	0.0815	3.929012346	3536.111111	3.536111111	35.36111111
7	0.0896	4.179012346	3761.111111	3.761111111	37.61111111
8	0.0965	4.391975309	3952.777778	3.952777778	39.52777778

Table 9: CDR% Calculation for F1 formulation.

Time	Absorbance	Concentration (µg)	Cumulative amount in 900ml	Cumulative concentration in mg	Cumulative % drug release
1	0.0165	1.922839506	1730.555556	1.730555556	17.30555556
2	0.028	2.277777778	2050	2.05	20.5
3	0.0395	2.632716049	2369.444444	2.369444444	23.69444444
4	0.054	3.080246914	2772.222222	2.772222222	27.72222222
5	0.0615	3.311728395	2980.555556	2.980555556	29.80555556
6	0.066	3.450617284	3105.555556	3.105555556	31.05555556
7	0.078	3.820987654	3438.888889	3.438888889	34.38888889
8	0.0815	3.929012346	3536.111111	3.536111111	35.36111111

Table 10: CDR% Calculation for F2 formulation.

Time	Absorbance	Concentration (µg)	Cumulative amount in 900ml	Cumulative concentration in mg	Cumulative % drug release
1	0.0055	1.583333333	1425	1.425	14.25
2	0.0175	1.953703704	1758.333333	1.758333333	17.58333333
3	0.019	2	1800	1.8	18
4	0.028	2.277777778	2050	2.05	20.5
5	0.029	2.308641975	2077.777778	2.077777778	20.77777778
6	0.0301	2.342592593	2108.333333	2.108333333	21.08333333
7	0.034	2.462962963	2216.666667	2.216666667	22.16666667
8	0.0401	2.651234568	2386.111111	2.386111111	23.86111111

Table 11: CDR% Calculation for F3 formulation.

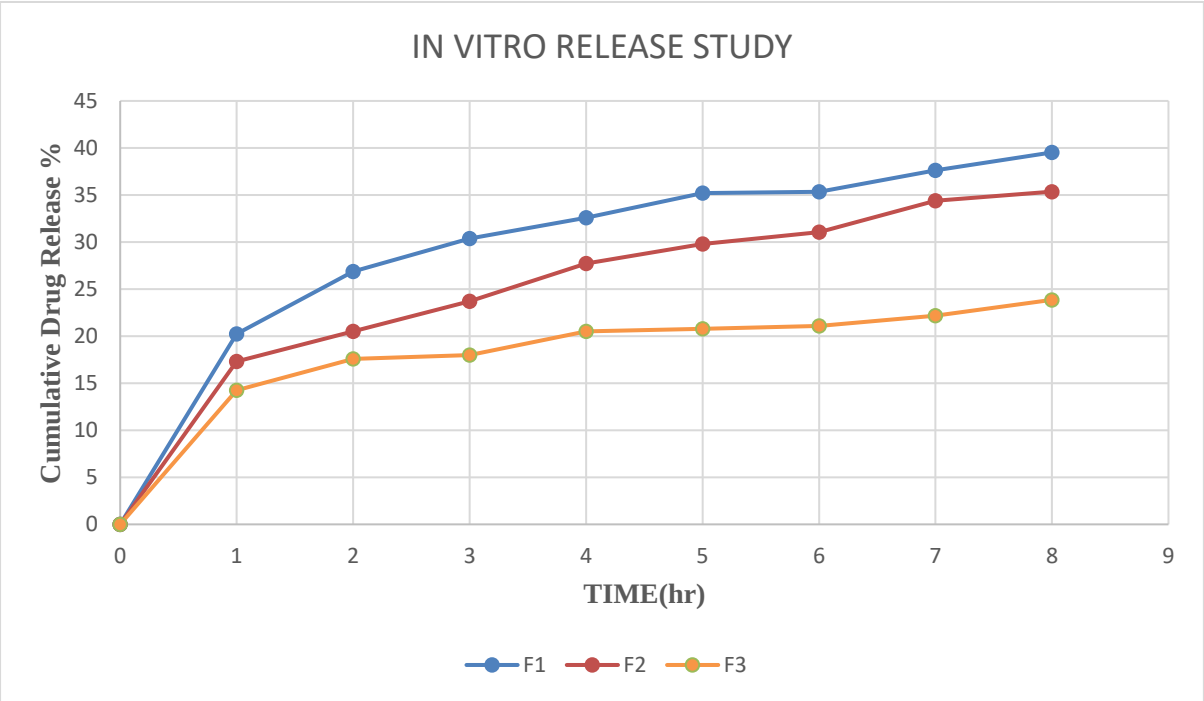

Figure 13: % Cumulative drug release vs. Time of F1, F2 and F3.

RELEASE KINETICS:

The release of a drug from the patch-based formulation depends on various underlying factors including, pH, temperature, drug solubility, polymer amount, drug diffusion through the polymeric matrix of the wafer, wafer's porosity and swelling index, and the water vapour transmission rate. Lyophilized wafer comprise of drug, and polymeric matrix where the drug is uniformly encapsulated inside the porous matrix structure, and the drug is released following some mechanism.

The Korsmeyer-Peppas model describes drug release from a polymeric system when the release mechanism is unknown. It is applied to the release profile to depict the diffusion type. After analyzing data obtained from Korsmeyer Peppas, it was observed that n values in all formulations are from 0.3585 to 0.2277, which fall in the range of $n \leq 0.45$, indicating Case I diffusion, also known as Fickian Diffusion. Here drug release mainly occurs due to diffusion through the pores present in the wafer, and it complies with first order. Data obtained by using First order equation, we observed R^2 values of release profiles of all formulations as 0.9846 to 0.9292, which shows acceptable linearity and also showed higher values than zero order.

The profiles obtained from the Higuchi model are linear as supported by the R^2 values (0.9919 - 0.9588). These values are higher than Hixson-Crowell establishing diffusion dominated release. Table 12 below presents the summary of R^2 value of various models of zero order kinetics, first order kinetic, Higuchi model, Hixon-Crowell model, Korsmeyer Peppas respectively.

SUMMARY:

FORMULATION	ZERO ORDER	FIRST ORDER	HIGUCHI	HIXSON-CROWELL	KORSMEYER-PEPPAS	
	R^2	R^2	R^2	R^2	R^2	n
F1	0.9143	0.9292	0.9704	0.9143	0.9839	0.3074
F2	0.9777	0.9846	0.9919	0.9777	0.9863	0.3585
F3	0.9229	0.935	0.9588	0.9229	0.9693	0.2277

Table 12: shows summary of R^2 value of different release kinetics model.

ZERO ORDER KINETICS:

Zero order: cumulative % drug release vs. time			
	FORMULATIONS		
TIME	F1	F2	F3
1	20.22222	17.30556	14.25
2	26.88889	20.5	17.58333
3	30.36111	23.69444	18
4	32.58333	27.72222	20.5
5	35.22222	29.80556	20.77778
6	35.36111	31.05556	21.08333
7	37.61111	34.38889	22.16667
8	39.52778	35.36111	23.86111

Table 13: shows calculation of zero order kinetics.

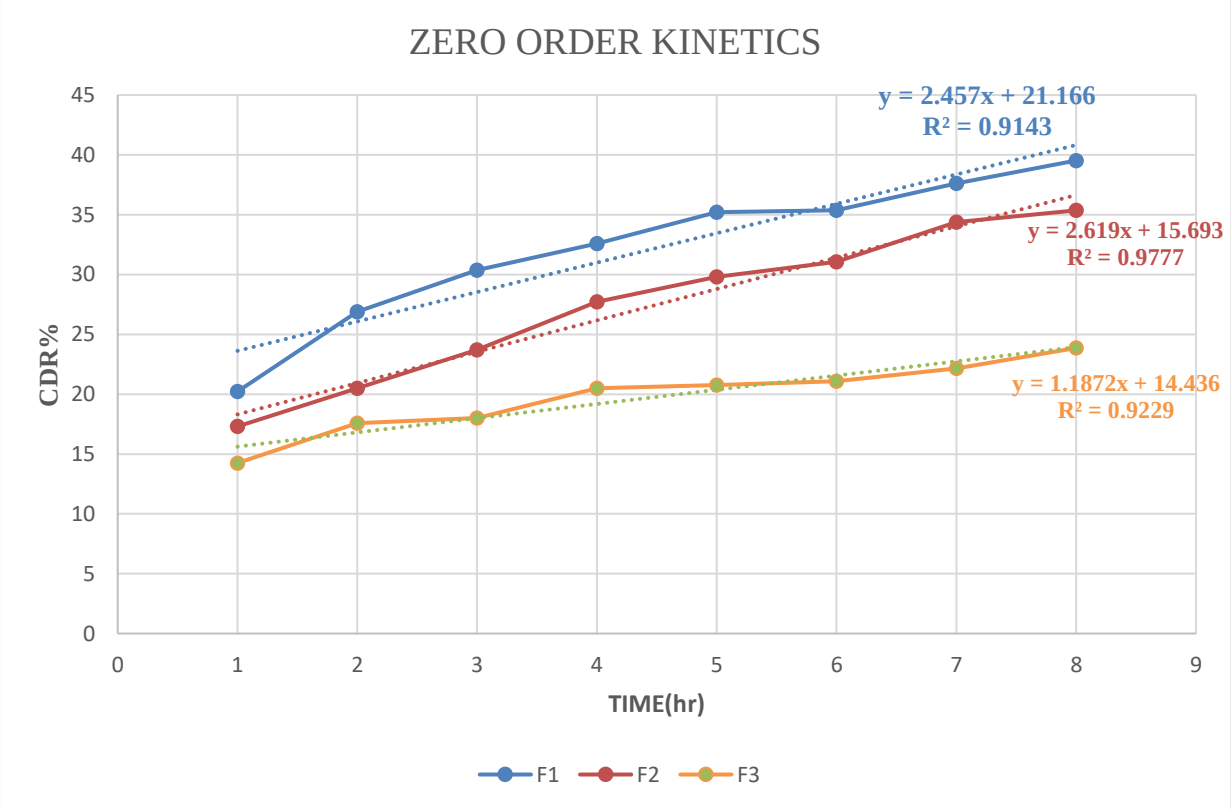

Figure 14: Shows zero order release kinetics of the wafers.

FIRST ORDER KINETICS:

First order: Log% drug remaining vs. time			
TIME	**FORMULATION**		
	F1	**F2**	**F3**
1	**1.901882**	**1.917476**	**1.933234**
2	**1.863983**	**1.900367**	**1.916015**
3	**1.842852**	**1.882556**	**1.913814**
4	**1.828767**	**1.859005**	**1.900367**
5	**1.811426**	**1.846303**	**1.898847**
6	**1.810494**	**1.838499**	**1.897169**
7	**1.795107**	**1.816977**	**1.891166**
8	**1.781556**	**1.810494**	**1.881607**

Table 14: Calculation for first order release kinetics

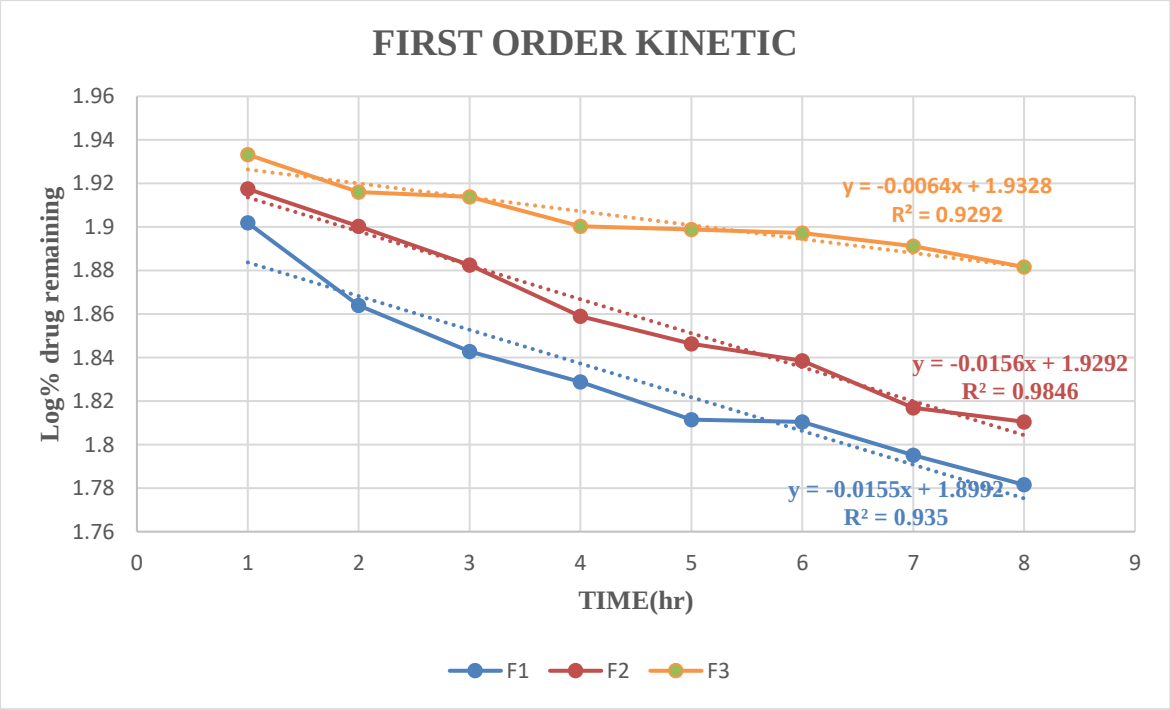

Figure 15: Shows first order release kinetics of the wafers.

HIGUCHI MODEL:

Higuchi: %CDR vs. sq. root of time:				
TIME		**FORMULATIONS**		
	SQ. ROOT OF TIME	**F1**	**F2**	**F3**
1	**1**	**20.22222**	**17.30556**	**14.25**
2	**1.414213562**	**26.88889**	**20.5**	**17.58333**
3	**1.732050808**	**30.36111**	**23.69444**	**18**
4	**2**	**32.58333**	**27.72222**	**20.5**
5	**2.236067977**	**35.22222**	**29.80556**	**20.77778**
6	**2.449489743**	**35.36111**	**31.05556**	**21.08333**
7	**2.645751311**	**37.61111**	**34.38889**	**22.16667**
8	**2.828427125**	**39.52778**	**35.36111**	**23.86111**

Table 15: Calculation for Higuchi model.

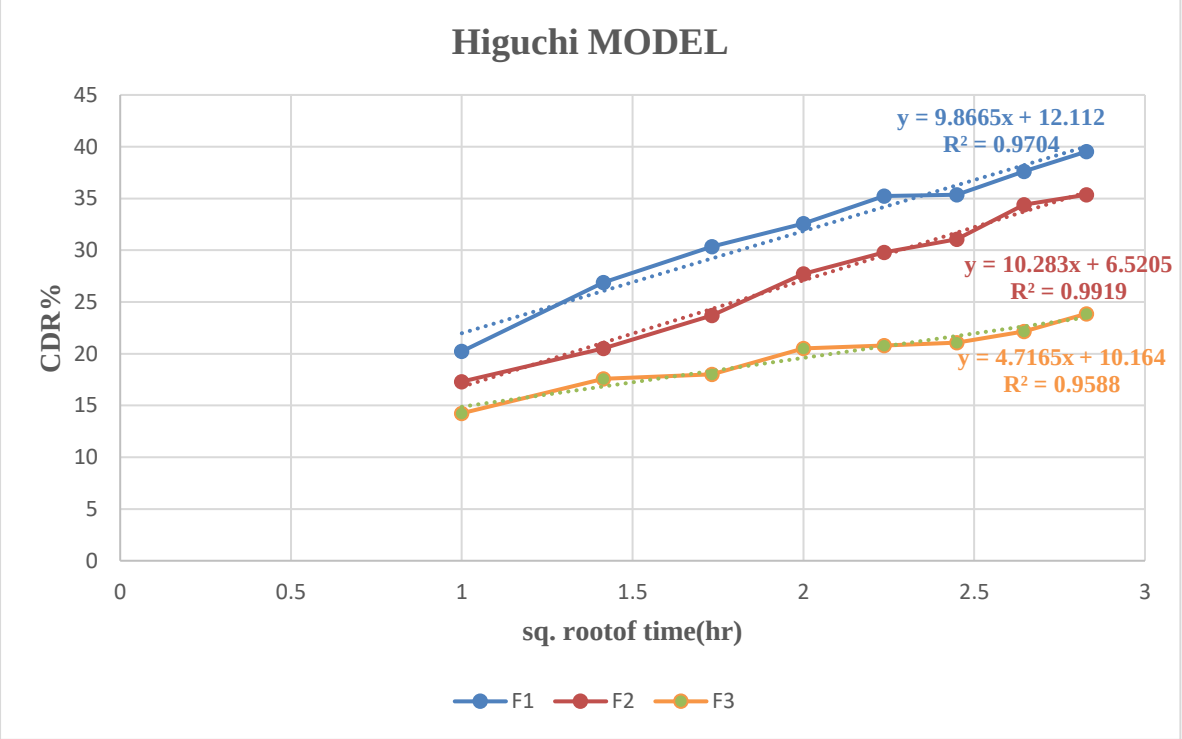

Figure 16: Shows Higuchi release kinetics model for wafers

HIXSON-CROWELL MODEL:

Hixson-Crowell: Cube root of % drug released vs. time:			
	CUBE ROOT OF % DRUG RELEASE		
TIME	F1	F2	F3
1	26.59259	27.56481	28.58333
2	24.37037	26.5	27.47222
3	23.21296	25.43519	27.33333
4	22.47222	24.09259	26.5
5	21.59259	23.39815	26.40741
6	21.5463	22.98148	26.30556
7	20.7963	21.87037	25.94444
8	20.15741	21.5463	25.37963

Table 16: Calculation for Hixson-Crowell model.

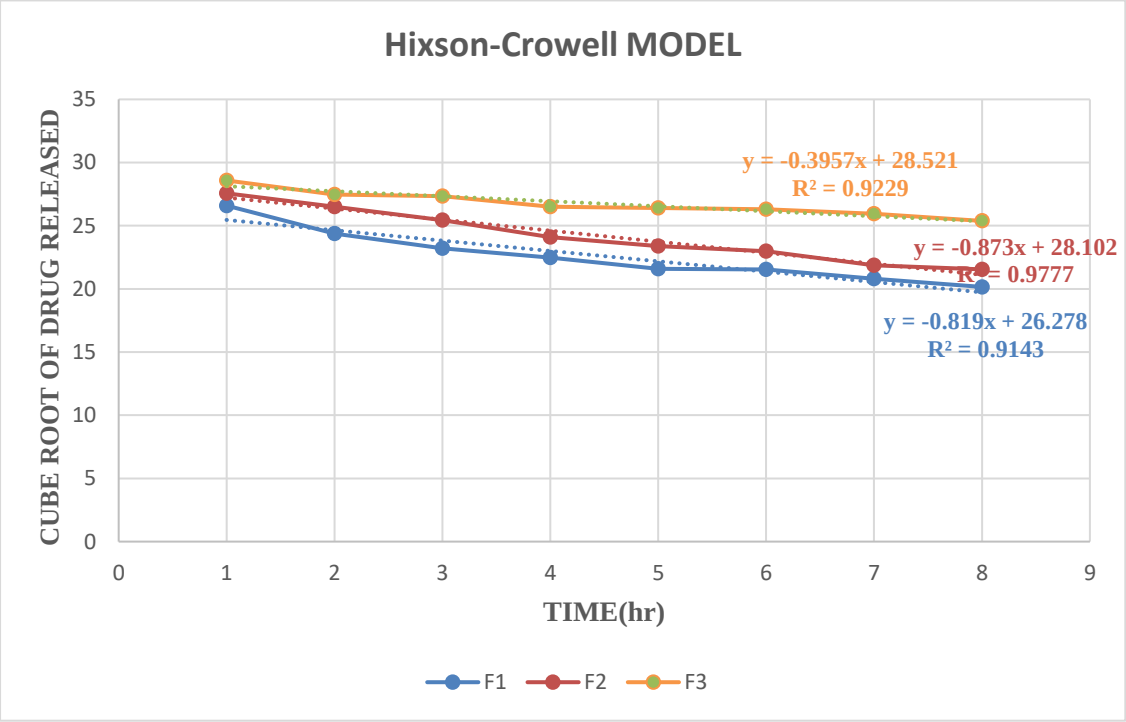

Figure 17: Shows Hixson-Crowell model.

KORSMEYER-PEPPAS MODEL:

Korsmeyer-Peppas: Log %CDR vs. Log time:			
	Log CDR (%)		
LOG TIME	F1	F2	F3
0	1.305829	1.238186	1.153815
0.30103	1.429573	1.311754	1.245101
0.477121	1.482318	1.374647	1.255273
0.60206	1.512996	1.442828	1.311754
0.69897	1.546817	1.474297	1.317599
0.778151	1.548526	1.492139	1.323939
0.845098	1.575316	1.536418	1.3457
0.90309	1.596902	1.548526	1.377691

Table 17: Calculation for Korsmeyer-Peppas model.

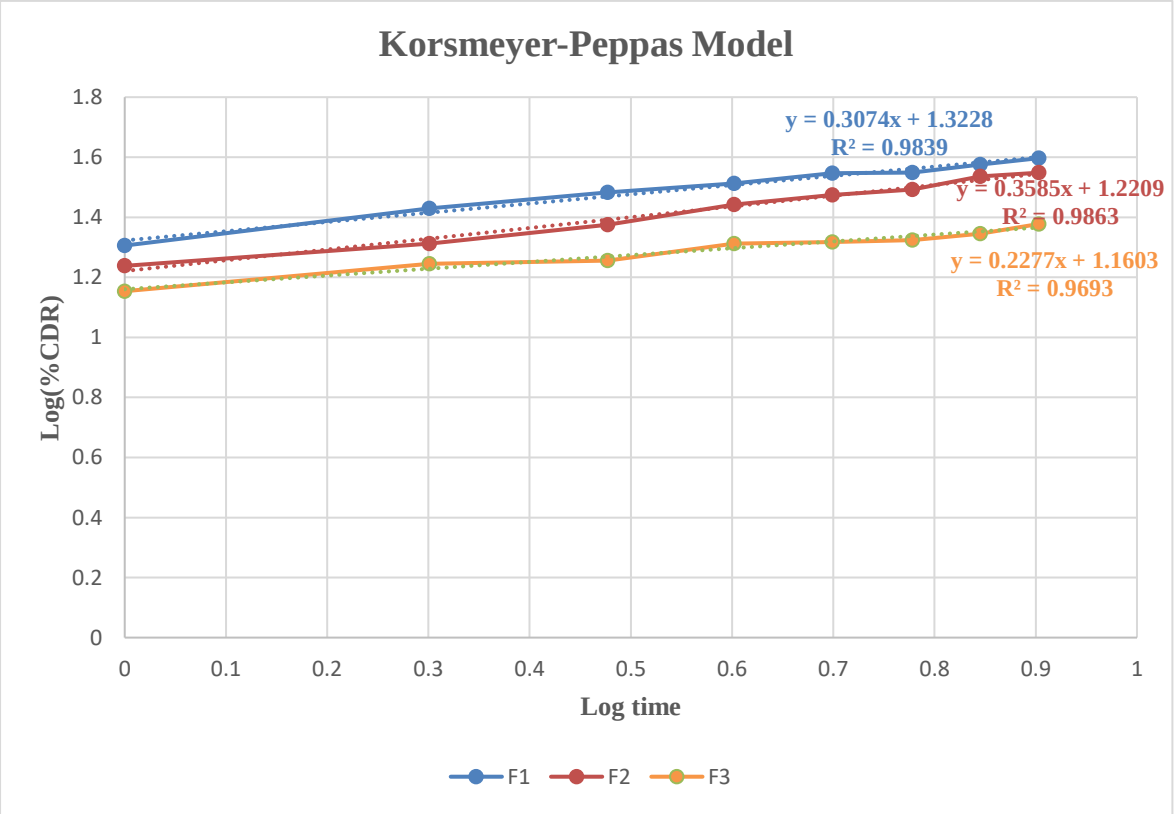

Figure 18: Shows Korsmeyer-Peppas release kinetics model.

CHAPTER 7:

CONCLUSION

7. SUMMARY AND CONCLUSION

The wound healing topically applied lyophilized wafers represent a significant advancement in the management of various chronic wound managements which represent a medical challenge because of various complicating factors including diabetes and malignancies, chronic systemic inflammation, persistent infection, destruction of neighbouring tissues, poor primary treatment and other patient-related factors such as poor nutrition. . The promising results from FTIR, SEM, and in vitro release studies underscore the potential of topical wafers as an effective and reliable treatment option. By offering enhanced drug delivery, sustained release, and a conducive healing environment, the wafer addresses the critical challenges associated with DFU (diabetic foot ulcer) treatment. Its ability to reduce infection risk and improve patient compliance further highlights its benefits. As research and development continue, this innovative approach holds great promise for improving the outcomes and quality of life for patients suffering from diabetic foot ulcers and venous leg ulcers (VLUs). The efficiency of these wafers in capturing and delivering drugs to specific targets depends on several physical parameters, including their wafer's encapsulation properties, porosity size, Water vapour transmission rate, and swelling index. The size of the porous complex matrix and release rate of drug can be adjusted by altering ratio of polymer and micro dispersing the polymeric solution. The hydrophilicity of the drug chosen for the encapsulation also depicts the easy of release into the target site. Additionally, physiological parameters such as the degree of wound, the amount of excudate, vascular supply, and underlying cronic diseases like diabetes mellitus and hypertension must also be taken into consideration when designing a drug loaded wafer. The synthesis of lyophilized wafer involves several methods, including forming a polymeric solution, drug dissolution, homogenisation, and lyophilization. These methods can be used to produce wafers of different porosity and tensile strength.

The synergistic effect localized magnetic hyperthermia shows promising results in treating diseases. The MNPs have great importance and are widely used in targeted drug delivery. As compared to conventional drug delivery, MNPs based drug delivery administration can minimize the doses of drugs and subsequently reduce the side effects.

Before preparation of drug loaded wafers for targeted drug delivery, pre-formulation studies are necessary for drug and polymers used in formulation. For the drug candidate melting point was determined and its solubility was assessed. The physical characteristics, melting point of curcumin was examined. The λmax of curcumin was determined and standard curve was plotted. Instrumental analysis (FTIR, and XRD) was performed for drug, blank and drug loaded wafers check any interaction among ingredients. Particle size, and morphology were also assessed by SEM. Various physical properties of the wafer was also determined to check for its compatibility for wounded target sites like folding endurance, WVTR and Swelling index. All of which showed promising results.

- Fourier Transform Infrared Spectroscopy (FTIR) analysis has confirmed the successful incorporation of drug (curcumin) within the lyophilized wafer. The characteristic peaks observed in the FTIR spectra indicate the presence of functional groups associated with the drug, and polymers ensuring their stability and compatibility within the wafer. This is crucial for maintaining the therapeutic efficacy of the wafer over time.

- Scanning Electron Microscopy (SEM) has provided detailed insights into the surface morphology and structural integrity of the transdermal patch. The SEM images reveal a uniform and porous structure, which is essential for controlled drug release and effective wound coverage. The porous nature of the wafer facilitates the sustained release of drug, enhancing the wound healing process by maintaining a moist environment and promoting cellular proliferation.

- In vitro release studies have demonstrated the wafer's ability to deliver drug in a controlled and sustained manner. The release profile indicates a steady release of the drug over an extended period, which is critical for managing chronic wounds such as DFUs. This controlled release mechanism ensures a consistent therapeutic effect, reducing the need for frequent wafer changes and improving patient compliance.

The future of topical wafers for wound healing is bright, with advancements in technology, personalized medicine, and regenerative techniques paving the way for more effective and efficient treatments. These innovations hold the potential to significantly improve the management of chronic wounds, such as diabetic foot ulcers, enhancing patient outcomes and quality of life. As research and development continue, we can expect topical patches or wafers to become an integral part of wound care, offering a versatile and powerful tool for healthcare providers.

CHAPTER 8:

REFERENCE.

REFERENCE

1. Patel, D., Patel, B. and Thakkar, H., 2021. Lipid based nanocarriers: promising drug delivery system for topical application. *European Journal of Lipid Science and Technology*, *123*(5), p.2000264.

2. Bhowmik, D., 2012. Recent advances in novel topical drug delivery system. *The Pharma Innovation*, *1*(9).

3. https://mobility-health.com/pages/skin-anatomy accessed on 31.07.2024

4. Powell, J., 2006. Skin physiology. *Women's Health Medicine*, *3*(3), pp.130-133.

5. Arda, O., Göksügür, N. and Tüzün, Y., 2014. Basic histological structure and functions of facial skin. *Clinics in dermatology*, *32*(1), pp.3-13.

6. Nair, A., Jacob, S., Al-Dhubiab, B., Attimarad, M. and Harsha, S., 2013. Basic considerations in the dermatokinetics of topical formulations. *Brazilian journal of pharmaceutical sciences*, *49*, pp.423-434.

7. https://nursing411.org/Courses/MD0575_Integumentar_System/5-05_Integum_Syst.html , accessed on 15.03.2024.

8. Simoes, A., Veiga, F. and Vitorino, C., 2019. Developing cream formulations: renewed interest in an old problem. *Journal of Pharmaceutical Sciences*, *108*(10), pp.3240-3251.

9. Mayba, J.N. and Gooderham, M.J., 2018. A guide to topical vehicle formulations. *Journal of Cutaneous Medicine and Surgery*, *22*(2), pp.207-212.

10. Ndukwe, G.I. and Chahul, H.F., 2016. Application and evaluation of Cucumeropsis mannii Naud. Seed oil in methyl salicylate liniment and salicylic acid lotion formulations. *Journal of Pharmacognosy and Phytochemistry*, *5*(5), pp.321-324.

11. https://burtsrx.com/types-topical-medications/ , accessed on 19.03.2024

12. Saroha, K., Yadav, B. and Sharma, B., 2011. Transdermal patch: A discrete dosage form. *Int J Curr Pharm Res*, *3*(3), pp.98-108.

13. Ahmed, A., Getti, G. and Boateng, J., 2018. Ciprofloxacin-loaded calcium alginate wafers prepared by freeze-drying technique for potential healing of chronic diabetic foot ulcers. *Drug Delivery and Translational Research*, *8*, pp.1751-1768.

14. 1. Pawar, H.V., Boateng, J.S., Ayensu, I. and Tetteh, J., 2014. Multifunctional medicated lyophilised wafer dressing for effective chronic wound healing. *Journal of Pharmaceutical Sciences*, *103*(6), pp.1720-1733.

15. 2. Ahmed, A., Getti, G. and Boateng, J., 2018. Ciprofloxacin-loaded calcium alginate wafers prepared by freeze-drying technique for potential healing of chronic diabetic foot ulcers. *Drug Delivery and Translational Research*, *8*, pp.1751-1768.

16. https://www.dowdevelopmentlabs.com/advantages-of-topical-drug-delivery-systems-a-closer-look/#:~:text=Unlike%20oral%20medications%20that%20circulate,and%20enhancing%20the%20therapeutic%20outcome.&text=Topical%20drug%20delivery%20excels%20in%20providing%20localized%20effects. Accessed on 09.07.2024

17. Patel, Pavan. (2022). A Review on Topical Drug Delivery System Patches. 7. 292-302. 10.35629/7781-0701292302.

18. Enoch, S. and Leaper, D.J., 2008. Basic science of wound healing. *Surgery (Oxford)*, *26*(2), pp.31-37.

19. Hunt, M., Torres, M., Bachar-Wikström, E. and Wikström, J.D., 2023. Multifaceted roles of mitochondria in wound healing and chronic wound pathogenesis. *Frontiers in Cell and Developmental Biology*, *11*, p.1252318.

20. Criollo-Mendoza, M.S., Contreras-Angulo, L.A., Leyva-López, N., Gutiérrez-Grijalva, E.P., Jiménez-Ortega, L.A. and Heredia, J.B., 2023. Wound healing properties of natural products: mechanisms of action. *Molecules*, *28*(2), p.598.

21. Leise, B.S., 2018. Topical wound medications. *Veterinary Clinics: Equine Practice*, *34*(3), pp.485-498.

22. Tenehaus, M. and Hans-Oliver, R., 2018. Topical agents and dressings for local burn wound care. *UpToDate. Available online: https://www. uptodate.*

com/contents/topical-agents-and-dressings-for-local-burn-wound-care (accessed on 3 February 2023).

23. Vitale, S., Colanero, S., Placidi, M., Di Emidio, G., Tatone, C., Amicarelli, F. and D'Alessandro, A.M., 2022. Phytochemistry and biological activity of medicinal plants in wound healing: an overview of current research. *Molecules*, *27*(11), p.3566.

24. Nadar, M.M. and Selvakumar, P.M., 2018. Plant-Derived Compounds for Wound Healing-A Review. *Organic & Medicinal Chemistry International Journal*, *5*(1), pp.13-17.

25. Okeke, O.C. and Boateng, J.S., 2017. Nicotine stabilization in composite sodium alginate based wafers and films for nicotine replacement therapy. *Carbohydrate polymers*, *155*, pp.78-88.

26. Matthews, K.H., Stevens, H.N.E., Auffret, A.D., Humphrey, M.J. and Eccleston, G.M., 2005. Lyophilised wafers as a drug delivery system for wound healing containing methylcellulose as a viscosity modifier. *International journal of pharmaceutics*, *289*(1-2), pp.51-62.

27. Matthews, K.H., Stevens, H.N.E., Auffret, A.D., Humphrey, M.J. and Eccleston, G.M., 2008. Formulation, stability and thermal analysis of lyophilised wound healing wafers containing an insoluble MMP-3 inhibitor and a non-ionic surfactant. *International journal of pharmaceutics*, *356*(1-2), pp.110-120.

28. Farias, S. and Boateng, J.S., 2018. Development and functional characterization of composite freeze dried wafers for potential delivery of low dose aspirin for elderly people with dysphagia. *International Journal of Pharmaceutics*, *553*(1-2), pp.65-83.

29. Ayensu, I., Mitchell, J.C. and Boateng, J.S., 2012. Development and physico-mechanical characterisation of lyophilised chitosan wafers as potential protein drug delivery systems via the buccal mucosa. *Colloids and Surfaces B: Biointerfaces*, *91*, pp.258-265.

30. Yadav, P.N., Bhat, P. and Soni, S., 2014. Glibenclamide fabricated transdermal wafers for therapeutic sustained delivery systems. *Int J Pharm Med Res*, *2*(2), pp.58-67.

31. Avachat, A.M. and Takudage, P.J., 2018. Design and characterization of multifaceted lyophilized liposomal wafers with promising wound healing potential. *Journal of Liposome Research*, *28*(3), pp.193-208.

32. Nagra, U., Barkat, K., Ashraf, M.U. and Shabbir, M., 2022. Feasibility of enhancing skin permeability of acyclovir through sterile topical lyophilized wafer on self-dissolving microneedle-treated skin. *Dose-Response*, *20*(2), p.15593258221097594.

33. Pawar, H.V., Boateng, J.S., Ayensu, I. and Tetteh, J., 2014. Multifunctional medicated lyophilised wafer dressing for effective chronic wound healing. *Journal of Pharmaceutical Sciences*, *103*(6), pp.1720-1733.

34. Akiyode, O. and Boateng, J., Composite biopolymer-based wafer dressings loaded with microbial biosurfactants for potential application in chronic wounds. Polymers. 2018; 10 (8).

35. Ghosal, K., Ranjan, A. and Bhowmik, B.B., 2014. A novel vaginal drug delivery system: anti-HIV bioadhesive film containing abacavir. *Journal of Materials Science: Materials in Medicine*, *25*(7), pp.1679-1689.

36. Ahmed, A., Getti, G. and Boateng, J., 2018. Ciprofloxacin-loaded calcium alginate wafers prepared by freeze-drying technique for potential healing of chronic diabetic foot ulcers. *Drug Delivery and Translational Research*, *8*, pp.1751-1768.

37. https://pubchem.ncbi.nlm.nih.gov/compound/Curcumin#section=Canonical-SMILES accessed on 29.07.2024

38. Zhai, K., Brockmüller, A., Kubatka, P., Shakibaei, M. and Büsselberg, D., 2020. Curcumin's beneficial effects on neuroblastoma: mechanisms, challenges, and potential solutions. *Biomolecules*, *10*(11), p.1469.

39. Liu, Z., Smart, J.D. and Pannala, A.S., 2020. Recent developments in formulation design for improving oral bioavailability of curcumin: a review. Journal of drug delivery science and technology, 60, p.102082.

40. Urošević, M., Nikolić, L., Gajić, I., Nikolić, V., Dinić, A. and Miljković, V., Curcumin: Biological Activities and Modern Pharmaceutical Forms. Antibiotics (Basel). 2022; 11 (2): 135.

41. https://www.rxlist.com/turmeric_curcumin/generic-drug.htm accessed on 29.07.2024

42. Jäger, R., Lowery, R.P., Calvanese, A.V., Joy, J.M., Purpura, M. and Wilson, J.M., 2014. Comparative absorption of curcumin formulations. *Nutrition journal*, *13*, pp.1-8.
43. AloK, A., Singh, I.D., Singh, S., Kishore, M. and Jha, P.C., 2015. Curcumin–pharmacological actions and its role in oral submucous fibrosis: a review. *Journal of clinical and diagnostic research: JCDR*, *9*(10), p.ZE01.
44. https://pubchem.ncbi.nlm.nih.gov/compound/Hydroxypropylmethylcellulose accessed on 29.07.2024
45. Deshmukh, K., Ahamed, M.B., Deshmukh, R.R., Pasha, S.K., Bhagat, P.R. and Chidambaram, K., 2017. Biopolymer composites with high dielectric performance: interface engineering. In *Biopolymer composites in electronics* (pp. 27-128). Elsevier.
46. https://www.excipia.eu/excipients/cellulose-derivatives/hypromellose/ accessed on 29.07.2024
47. https://www.medchemexpress.com/Hypromellose.html#:~:text=HPMC%20(Synonyms%3A%20Hypromellose%3B%20(,methyl%20cellulose%3B%20Celacol%20HPM%205000)&text=HPMC%20(Hypromellose)%20is%20a%20hydrophilic,to%20form%20swellable%2Dsoluble%20matrices. Accessed on 29.07.2024
48. https://pubchem.ncbi.nlm.nih.gov/compound/Ethyl-cellulose. Accessed on 29.07.2024
49. https://www.fao.org/fileadmin/user_upload/jecfa_additives/docs/Monograph1/additive-178-m1.pdf
50. https://www.chemwhat.com/ethyl-cellulose-cas-9004-57-3/ accessed on 29.07.2024
51. https://pubchem.ncbi.nlm.nih.gov/compound/N-Vinyl-2-pyrrolidone accessed on 29.07.2024
52. https://brmchemicals.com/products/polyvinylpyrrolidone-k-30-p-v-p-k-30 accessed on 29.07.2024
53. http://www.sellchems.com/products/fine-chemical/polyvinylpyrrolidone-cas-9003-39-8/ accessed on 29.07.2024
54. Kurakula, M. and Rao, G.K., 2020. Pharmaceutical assessment of polyvinylpyrrolidone (PVP): As excipient from conventional to controlled delivery systems with a spotlight on COVID-19 inhibition. *Journal of drug delivery science and technology*, *60*, p.102046.
55. http://www.chemspider.com/Chemical-Structure.682.html accessed on 29.07.2024
56. https://pubchem.ncbi.nlm.nih.gov/compound/Ethanol accessed on 29.07.2024

57. https://chem.libretexts.org/Courses/Purdue/Purdue%3A_Chem_26505%3A_Organic_Chemistry_I_(Lipton)/Chapter_4._Intermolecular_Forces_and_Physical_Properties/4.4_Solubility on 29.07.2024
58. https://www.toppr.com/guides/chemistry/organic-chemistry/chloroform/#:~:text=Its%20chemical%20formula%20is%20CHCl,reaching%20the%20very%20high%20temperatures. Accessed on 30.07.2024
59. https://www.vedantu.com/question-answer/chloroform-is-used-a-as-a-general-anesthetic-b-class-11-chemistry-cbse-5ff361c1330feb57429ef4d0 accessed on 30.07.2024
60. https://pubchem.ncbi.nlm.nih.gov/compound/Chloroform accessed on 30.07.2024
61. Snow, J., 1955. On chloroform and other anaesthetics: their action and administration. *British journal of anaesthesia*, *27*(10), pp.498-511.
62. https://www.acs.org/molecule-of-the-week/archive/p/potassium-dihydrogen-phosphate.html accessed on 31.07.2024
63. https://pubchem.ncbi.nlm.nih.gov/compound/Potassium-dihydrogen-phosphate accessed on 31.07.2024
64. https://www.chembk.com/en/chem/Potassium%20dihydrogen%20phosphate accessed on 31.07.2024
65. https://pubchem.ncbi.nlm.nih.gov/compound/Disodium-hydrogen-phosphate accessed on 31.07.2024
66. https://www.geeksforgeeks.org/sodium-hydrogen-phosphate-formula-structure-properties-uses-sample-questions/ accessed on 31.07.2024
67. https://www.pharmaexcipients.com/product/di-sodium-hydrogen-phosphate-dihydrate-emprove-expert/ accessed on 31.07.2024
68. https://pubchem.ncbi.nlm.nih.gov/compound/Sodium-Chloride accessed on 31.07.2024
69. https://infinitylearn.com/surge/sodium-chloride-formula/ accessed on 31.07.2024
70. Nurahmanto, D., 2013. Development and validation of UV spectrophotometric method for quantitative estimation of Promethazine HCl in phosphate buffer saline pH 7.4. *International Current Pharmaceutical Journal*, *2*(8), pp.141-142.
71. Majumder, K.K., Sharma, J.B., Kumar, M., Bhatt, S. and Saini, V., 2020. Development and validation of UV-Visible spectrophotometric method for the estimation of curcumin in bulk and pharmaceutical formulation. *Pharmacophores*, *10*(1), pp.115-21.

72. Kahali, N., Khanam, J. and Chatterjee, H., 2022. An overview of preparation and characterization of solid binary system and its application on transdermal film with variation of plasticizers. *Brazilian Journal of Pharmaceutical Sciences*, *58*, p.e191123.
73. Ghosal, K., Ranjan, A. and Bhowmik, B.B., 2014. A novel vaginal drug delivery system: anti-HIV bioadhesive film containing abacavir. *Journal of Materials Science: Materials in Medicine*, *25*(7), pp.1679-1689.
74. Ramadan, E., Borg, T., Abdelghani, G. and Saleh, N.M., 2016. Transdermal microneedle-mediated delivery of polymeric lamivudine-loaded nanoparticles. *J. Pharm. Technol. Drug Res*, *5*(1), p.1.
75. Okeke, O.C. and Boateng, J.S., 2017. Nicotine stabilization in composite sodium alginate based wafers and films for nicotine replacement therapy. *Carbohydrate polymers*, *155*, pp.78-88.
76. Huang, J. and Chen, Y., 2010. Effects of air temperature, relative humidity, and wind speed on water vapor transmission rate of fabrics. *Textile research journal*, *80*(5), pp.422-428.
77. Basha, R.K., Konno, K., Kani, H. and Kimura, T., 2011. Water vapor transmission rate of biomass based film materials. *Engineering in Agriculture, Environment and Food*, *4*(2), pp.37-42.
78. Marioane, C.A., Bunoiu, M., Mateescu, M., Sfîrloagă, P., Vlase, G. and Vlase, T., 2021. Preliminary study for the preparation of transmucosal or transdermal patches with acyclovir and lidocaine. *Polymers*, *13*(20), p.3596.
79. Maurizii, G., Moroni, S., Khorshid, S., Aluigi, A., Tiboni, M. and Casettari, L., 2023. 3D-printed EVA-based patches manufactured by direct powder extrusion for personalized transdermal therapies. *International Journal of Pharmaceutics*, *635*, p.122720.
80. Ramos, P., Raczak, B.K., Silvestri, D. and Wacławek, S., 2023. Application of TGA/c-DTA for distinguishing between two forms of naproxen in pharmaceutical preparations. *Pharmaceutics*, *15*(6), p.1689.
81. Ahmed, A., Getti, G. and Boateng, J., 2018. Ciprofloxacin-loaded calcium alginate wafers prepared by freeze-drying technique for potential healing of chronic diabetic foot ulcers. *Drug Delivery and Translational Research*, *8*, pp.1751-1768.

82. Pawar, H.V., Boateng, J.S., Ayensu, I. and Tetteh, J., 2014. Multifunctional medicated lyophilised wafer dressing for effective chronic wound healing. *Journal of Pharmaceutical Sciences*, *103*(6), pp.1720-1733.
83. Ayensu, I., Mitchell, J.C. and Boateng, J.S., 2012. Development and physico-mechanical characterisation of lyophilised chitosan wafers as potential protein drug delivery systems via the buccal mucosa. *Colloids and Surfaces B: Biointerfaces*, *91*, pp.258-265.
84. Ng, S.F. and Jumaat, N., 2014. Carboxymethyl cellulose wafers containing antimicrobials: A modern drug delivery system for wound infections. *European Journal of Pharmaceutical Sciences*, *51*, pp.173-179.
85. https://www.mt.com/in/en/home/applications/Application_Browse_Laboratory_Analytics/Thermal_Values/melting-point-determination.html#:~:text=Melting%20points%20are%20often%20used,exhibit%20a%20large%20melting%20interval. Accessed on 31.07.2024
86. https://www.mt.com/ch/fr/home/library/applications/lab-analytical-instruments/melting-point-of-curcumin.html#:~:text=Curcumin%20(E100)%20is%20used%20in,%C2%B0C%20%E2%80%93%20182%C2%B0C. Accessed on 31.07.2024
87. Nagesh, G., Santosh, J., Audumbar, M. and Manojkumar, P., 2016. A review on recent trends in oral drug delivery-lyophilized wafer technology. *Int J Res Pharm and Pharm Sci*, *1*, pp.5-9
88. Farias, S. and Boateng, J.S., 2018. Development and functional characterization of composite freeze dried wafers for potential delivery of low dose aspirin for elderly people with dysphagia. *International Journal of Pharmaceutics*, *553*(1-2), pp.65-83.
89. Sekharan, T.R., Chandira, R.M., Rajesh, S.C., Tamilvanan, S., Vijayakumar, C.T. and Venkateswarlu, B.S., 2021. Stability of curcumin improved in hydrophobic based deep eutectic solvents. *Research Journal of Pharmacy and Technology*, *14*(12), pp.6430-6436.
90. https://www.researchgate.net/publication/363842679_Effect_of_Hydrophobic_Powders_on_the_Tensile_Strength_of_the_Tablet accessed on 05.08.2024

91. Rezvanian, M., Tan, C.K. and Ng, S.F., 2016. Simvastatin-loaded lyophilized wafers as a potential dressing for chronic wounds. *Drug development and industrial pharmacy*, *42*(12), pp.2055-2062.
92. Roy, S. and Rhim, J.W., 2020. Preparation of bioactive functional poly (lactic acid)/curcumin composite film for food packaging application. *International Journal of Biological Macromolecules*, *162*, pp.1780-1789.
93. Alzainy, A. and Boateng, J., 2022. Novel mucoadhesive wafers for treating local vaginal infections. *Biomedicines*, *10*(12), p.3036.
94. Darandale, S.S. and Vavia, P.R., 2013. Cyclodextrin-based nanosponges of curcumin: formulation and physicochemical characterization. *Journal of inclusion phenomena and macrocyclic chemistry*, *75*, pp.315-322.
95. Huang, L.Y., Yu, D.G., Branford-White, C. and Zhu, L.M., 2012. Sustained release of ethyl cellulose micro-particulate drug delivery systems prepared using electrospraying. *Journal of Materials Science*, *47*, pp.1372-1377.
96. Shetty, G.R., Rao, B.L., Asha, S., Wang, Y. and Sangappa, Y., 2015. Preparation and characterization of silk fibroin/hydroxypropyl methyl cellulose (HPMC) blend films. *Fibers and Polymers*, *16*, pp.1734-1741.
97. Erkoç, T., Sevgili, L.M. and Çavuş, S., 2022. Hydroxypropyl cellulose/polyvinylpyrrolidone matrix tablets containing ibuprofen: infiltration, erosion and drug release characteristics. *ChemistrySelect*, *7*(30), p.e202202180.
98. Akiyode, O. and Boateng, J., 2018. Composite biopolymer-based wafer dressings loaded with microbial biosurfactants for potential application in chronic wounds. *Polymers*, *10*(8), p.918.
99. Snetkov, P., Rogacheva, E., Kremleva, A., Morozkina, S., Uspenskaya, M. and Kraeva, L., 2022. In-vitro antibacterial activity of curcumin-loaded nanofibers based on hyaluronic acid against multidrug-resistant ESKAPE pathogens. *Pharmaceutics*, *14*(6), p.1186.